



Royal Netherlands  
Meteorological Institute  
*Ministry of Infrastructure and the  
Environment*

# Estimation of advective fluxes from CO<sub>2</sub> flux profile observations at the Cabauw Tower

Kasper O. Gerritsen

De Bilt , 2012 | Technical Report ; TR-330



# Estimation of advective fluxes from CO<sub>2</sub> flux profile observations at the Cabauw Tower

Version 1.0

Date April 2012  
Status Final



# Estimation of Advective Fluxes from CO<sub>2</sub> Flux Profile Observations at the Cabauw Tower



**Master of Science Thesis**

**Kasper O. Gerritsen**

Climate Studies – Earth System Science track - Wageningen University

April 2012

Royal Netherlands Meteorological Institute  
Regional Climate Division

Wageningen University  
Earth System Science Group

*supervisor:* Dr. Fred C. Bosveld

*supervisor:* Dr. ir. Laurens N. Ganzeveld



## **ABSTRACT**

The exchange of carbon dioxide (CO<sub>2</sub>) between the atmosphere and the terrestrial biosphere is an important link in climate related research. In this field of research, there is a need to quantify regional scale vertical fluxes of CO<sub>2</sub> to bridge the gap between ecosystem scale and the global scale. These regional scale fluxes may be obtained by accurate observations higher up in the atmosphere. In doing so, complicating factors arise such as storage of CO<sub>2</sub> beneath the level of observation and advection. The question of advective contribution to the net ecosystem exchange (*NEE*) of CO<sub>2</sub> is investigated at the 213 m tall-tower near Cabauw, The Netherlands. In addition, vertical and temporal variability of CO<sub>2</sub> at Cabauw is studied. This site is particularly interesting because advection is assumed to be small under convective conditions, because of the relatively homogeneous and flat surrounding landscape. Moreover, the Cabauw tower is equipped with CO<sub>2</sub> flux and concentration instrumentation at several levels, which enables detailed advection estimations based on a scalar budget methodology. To judge advection under convective conditions a summer half year was studied. During monthly averaged diurnal cycles the advective contribution to *NEE* was found to be in the order of 20%, but also showed a significantly noisy signal in general. The advection is typically alternately CO<sub>2</sub> enriching and depleting. However, with a fairly constant easterly wind direction over the course of a month the advective contribution was observed to be persistently and significantly enriching during daytime. This is probably related to the presence of a village in the footprint of the flux observations. This study shows that in assessments of *NEE* for Cabauw and similar landscapes advection should be considered.



# TABLE OF CONTENTS

<b>ABSTRACT .....</b>	<b>v</b>
<b>1. INTRODUCTION .....</b>	<b>1</b>
<b>2. THEORY AND METHODS .....</b>	<b>3</b>
2.1. THE CABAUW MEASUREMENT SITE .....	3
2.2. CO <sub>2</sub> ADVECTION: SCALAR BUDGET METHODOLOGY .....	4
2.3. MEASUREMENTS AND COMPUTATIONS .....	7
2.3.1. VERTICAL TURBULENT FLUX (EDDY COVARIANCE FLUX) (F <sub>EC</sub> ) .....	7
2.3.2. CONCENTRATION AND STORAGE FLUX (F <sub>ST</sub> ) .....	8
2.3.3. NET ECOSYSTEM EXCHANGE (NEE) AND ADVECTIVE FLUX (ΔNEE) .....	9
2.3.4. WIND DIRECTION AND SHORT WAVE DOWN RADIATION .....	9
2.4. DATA SELECTION, FILTERING AND CLEANING .....	9
2.5. FOOTPRINTS AND CO <sub>2</sub> SOURCES/SINKS .....	11
2.6. MODELLING NET ECOSYSTEM EXCHANGE .....	12
<b>3. RESULTS .....</b>	<b>15</b>
3.1. DIURNAL CYCLE OF CO <sub>2</sub> CONCENTRATIONS AND FLUXES .....	15
3.1.1. CONCENTRATION .....	15
3.1.2. FLUXES .....	19
3.1.3. NET ECOSYSTEM EXCHANGE .....	25
3.2. ADVECTION .....	29
3.2.1. MONTHLY AND 3-MONTHLY AVERAGED DIURNAL CYCLES OF ΔNEE .....	29
3.2.2. ΔNEE VERSUS WIND DIRECTION .....	39

3.2.3. ATTRIBUTING ADVECTION TO STORAGE AND TURBULENT FLUX .....	44
3.2.4. CONCENTRATION VERSUS WIND DIRECTION .....	45
3.2.5. SOURCE AND SINK AREAS .....	48
<b>4. DISCUSSION AND CONCLUSIONS .....</b>	<b>51</b>
4.1. CO <sub>2</sub> CONCENTRATION .....	51
4.2. CO <sub>2</sub> FLUXES .....	52
4.3. CO <sub>2</sub> NET ECOSYSTEM EXCHANGE .....	53
4.4. CO <sub>2</sub> ADVECTION .....	53
<b>ACKNOWLEDGEMENTS.....</b>	<b>57</b>
<b>REFERENCES .....</b>	<b>59</b>

# 1. INTRODUCTION

Carbon dioxide (CO<sub>2</sub>) exchange between the land surface and the atmosphere constitutes a significant component of the carbon cycle. It co-regulates the atmospheric CO<sub>2</sub> content, and therefore relates directly to climate change. On the global scale, the current role of the terrestrial system is reasonably understood. The terrestrial biosphere, in general - acting as a net sink for CO<sub>2</sub> - partly offsets anthropogenic CO<sub>2</sub> emissions [Davis *et al.*, 2003]. Yet, regarding present and future climate states there is a need to better understand and quantify the feedbacks between the biosphere and the climate [Friedlingstein *et al.*, 2003]. Therein, long-term data collection at the ecosystem scale is crucial; in order to quantify representative land surface-atmosphere carbon transfer and to find its causes, ranging from local to global scale. These findings can ultimately provide more accurate explanations of trends and patterns in the atmospheric CO<sub>2</sub> burden, and improve our understanding of this part of the climate system [Wilson and Baldocchi, 2001; Yi *et al.*, 2000; Davis *et al.*, 2003].

In this field of research the quantity of main interest is the net ecosystem-atmosphere exchange (*NEE*) of CO<sub>2</sub>, which is the combined result of photosynthetic CO<sub>2</sub> uptake and CO<sub>2</sub> release due to respiration processes. Using the typical sign convention, the *NEE* is ecologically defined as [Davis *et al.*, 2003]:

$$NEE = RE - GEP \quad (1),$$

where *RE* stands for total ecosystem respiration and *GEP* is the gross ecosystem productivity. A positive *NEE* means a net CO<sub>2</sub> release into the atmosphere, whereas a negative value implies a net uptake of CO<sub>2</sub>. The *NEE* can be investigated on the ecosystem scale by measuring CO<sub>2</sub> vertical turbulent fluxes close to the surface. Vertical turbulent fluxes are usually calculated using eddy covariance methods. A global network of these flux sites, *FLUXnet*, has been established with a focus on international collaboration [Baldocchi *et al.*, 2001]. To bridge the gap between ecosystem scale and regional scale, either airplane-based or tall tower-based observations are used. Observations at higher levels in the atmosphere “see” a larger footprint, but complicated aspects arise, such as storage of CO<sub>2</sub> below the level of observation and an increasing influence of advection. The Cabauw tower, with its extensive instrumentation and relatively ideal surroundings, serves as a nice test-bed to judge the potential of such regional scale flux observation techniques.

It is often assumed that CO<sub>2</sub> advection is negligible if: 1) the atmospheric boundary layer is convective, 2) the landscape surrounding the tower and its sources and sinks for CO<sub>2</sub> are relatively homogeneous, and

3) the terrain is reasonably flat [Yi *et al.*, 2000; Casso-Torralba *et al.*, 2008]. In that case, the *NEE* is assumed to be estimated reasonably well by the summation of the vertical turbulent flux and the storage flux below the level of turbulent flux observation:

$$NEE_0 = F_{ST} + F_{EC} \quad (2)$$

Here, the storage flux is denoted by  $F_{ST}$  and the vertical turbulent flux by  $F_{EC}$ . The subscript zero is added to *NEE* to distinguish it from a more accurate expression for *NEE*, which in principle should also include the advective component. By applying this method at different heights the hypothesis of no advection can in principle be tested. At Cabauw, CO<sub>2</sub> flux observations and CO<sub>2</sub> concentration measurements at different heights are available. Moreover, landscape conditions at the Cabauw measurement site are ideal for testing this assumption, because of negligible height differences and a vegetation cover on the regional scale consisting mainly of grass.

A full year of data is studied, being: July 2007-June 2008. The study starts with a description of temporal and vertical variability in CO<sub>2</sub> concentrations and vertical turbulent fluxes, with a focus on diurnal and seasonal cycles. Then, the study proceeds with the estimation of persistent advective flux, because the persistency will have a significant effect when integrating  $NEE_0$  over longer time scales. To estimate advection a scalar budget method for CO<sub>2</sub> is used, which is adopted from Yi *et al.* [2000] and presented with diurnal cycles averaged over 1-month and 3-month periods. The potential causes of advection are then investigated using footprint estimations. Additionally, observational  $NEE_0$  data are compared to model based *NEE* data in this investigation.

Preliminary studies at Cabauw by Werner *et al.* [2004] and Casso-Torralba *et al.* [2008] already suggested a significant contribution by advection, also during convective daytime situations. Werner *et al.* studied monthly averages for September 2003 and April 2004, whereas Casso-Torralba *et al.* investigated advection on a daily basis. In this investigation, using a larger data set, the validity of the previously mentioned assumption [ $NEE = NEE_0$ ] is tested for Cabauw. These findings may also be valid for ecosystems in a landscape setting similar to Cabauw. The primary research questions to be answered here are:

- i) *Can CO<sub>2</sub> advection be significantly observed at Cabauw under convective conditions?*
- ii) *What are the potential causes of advection?*
- iii) *Is there a major and persistent contribution to the CO<sub>2</sub> budget associated with advection?*

## 2. THEORY AND METHODS

### 2.1. THE CABAUW MEASUREMENT SITE

The 213 m high Cabauw mast is located in the western part of The Netherlands (51.971 °N, 4.927 °E). It was specifically built for meteorological research and air pollution studies and has been operational since 1973 [Van Ulden and Wieringa, 1995]. The location was chosen because of its representativeness for the landscape of this part of The Netherlands, which is dominated by nearly flat grassy meadows on clay and peat soils. An additional reason was that only minor landscape developments were planned in this region [Van Ulden and Wieringa, 1995]. Indeed, no major land-use changes did occur in the immediate surroundings up to and including the period under study (2007-2008). At present, the only noteworthy change has come from the westwards expansion of the town of Lopik. The surroundings can be seen below in Figure 1, showing a satellite image (Aerodata, 2011) from 2007 centered overhead the mast (yellow marker indicates position of mast). The lateral distance between the mast and the edge of the picture is about 2.5 km.

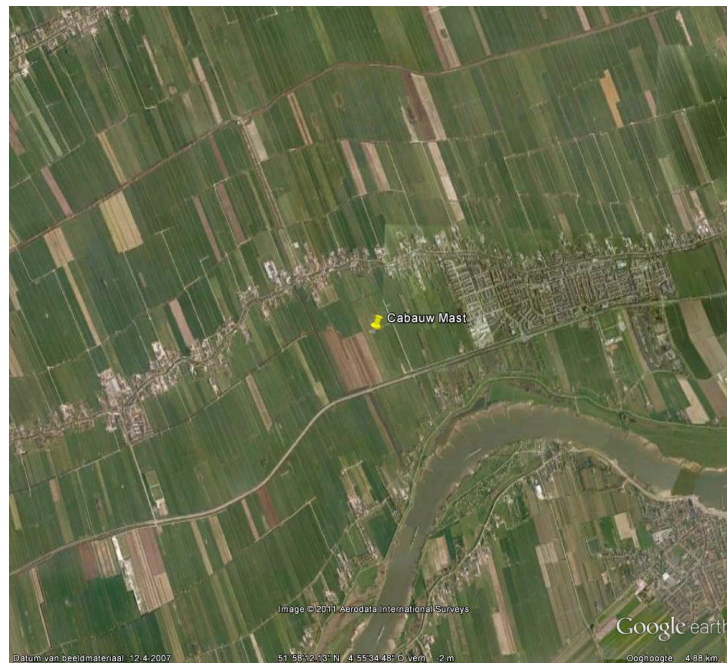


Figure 1. Satellite image obtained from Google Earth showing the Cabauw surroundings. Picture taken on April 12<sup>th</sup> 2007. Lateral distance from the mast (indicated by yellow marker) to the edge of the image is about 2.5 km. North is up. Aerodata, 2011.

Directly surrounding the measurement site the land is agricultural with meadows and ditches for at least 400 m in all directions. Open pasture extends towards the west-southwest for about 2 km. The town of Lopik lies to the east at approximately 500-700 m. The town of Cabauw is the elongated urban area west of the mast, visible in Figure 1. In south-easterly directions some orchards exist. Behind this patch lies the river Lek and some relatively heterogeneous land cover. At the site the grassy vegetation cover is nearly 100% all year round, showing virtually no bare soil. The dominant grass specie is *Lolium perenne*, but lesser amounts of *Poa trivialis* and *Alopecurus geniculatus* grow in the surrounding region [Beljaars and Bosveld, 1996].

At present, the Cabauw Experimental Site for Atmospheric Research (*CESAR*) is the focal point for experimental atmospheric research in The Netherlands. Besides the mast itself, the site comprises additional fields housing further *in-situ* sensors, and a field with ground-based remote sensing instruments for profiling of the atmospheric column over the site. Many meteorological, climatological and hydrological parameters are observed at *CESAR*. The site serves fundamental atmospheric studies, model evaluation, satellite validation, climate monitoring and e.g. greenhouse gas measurements. It is also part of project *ICOS*, which stands for Integrated Carbon Observation System. This is a European partnership to understand and quantify the greenhouse balance of the European continent and adjacent regions, using a network of tall towers, ecosystem flux sites and aircraft-based observations [online documentation – *ICOS*, 2011].

Five research institutes and three universities collaborate at Cabauw. The Royal Netherlands Meteorological Institute (*KNMI*) provides the CO<sub>2</sub> turbulent flux data for this thesis. However, turbulent flux observations at 100 m height are done with instruments from the *Alterra* research institute, Wageningen. CO<sub>2</sub> concentration measurements are managed by the Energy Research Center of the Netherlands (*ECN*). All measurement data are distributed to *KNMI* via a permanent data-link and stored in the *MOBIBASE* database [online documentation – *Bosveld*, 2010]. At *KNMI*, where this thesis work was conducted, the data analysis is performed using *MOBIBASE* software [online documentation – *Bosveld*, 2010].

## 2.2. CO<sub>2</sub> ADVECTION: SCALAR BUDGET METHODOLOGY

A scalar budget methodology is used in order to quantify the advection of CO<sub>2</sub> at Cabauw. The theoretical derivation of this mass conservation approach is given in this section.

The conservation equation for a scalar quantity  $c$ , such as  $\text{CO}_2$ , reads as [Yi *et al.*, 2000]:

$$\frac{\partial c}{\partial t} + u \frac{\partial c}{\partial x} + w \frac{\partial c}{\partial z} = v_c \left( \frac{\partial^2 c}{\partial x^2} + \frac{\partial^2 c}{\partial z^2} \right) + s_c \quad (3)$$

Here  $x$  is aligned with the horizontal mean wind direction,  $z$  is perpendicular to the long-term average streamlines at the Cabauw mast, and thus virtually perpendicular to the surface of the site terrain,  $u$  and  $w$  are the velocities in the  $x$  and  $z$  directions respectively, and  $v_c$  is the molecular diffusivity. The final term  $s_c$  on the right-hand side of equation (3) is a source term, which for  $\text{CO}_2$  is negligible above vegetation height [Yi *et al.*, 2000]. This height for Cabauw approximates the land surface, because of the short grassy vegetation. Therefore, a reasonable simplification can be applied by removing  $s_c$  from equation (3). Then, applying Reynolds decomposition, averaging and introducing the turbulent continuity equation yields [Yi *et al.*, 2000]:

$$\frac{\partial \bar{c}}{\partial t} + \bar{u} \frac{\partial \bar{c}}{\partial x} + \bar{w} \frac{\partial \bar{c}}{\partial z} + \frac{\partial \overline{u'c'}}{\partial x} + \frac{\partial \overline{w'c'}}{\partial z} = v_c \left( \frac{\partial^2 \bar{c}}{\partial x^2} + \frac{\partial^2 \bar{c}}{\partial z^2} \right) \quad (4)$$

Reynolds averaging is denoted by an overbar and prime values indicate the instantaneous deviations from the mean quantities. The final two terms on the left-hand side of equation (4) are thus the horizontal and vertical flux divergence, respectively. The first term on the right-hand side of equation (4) is molecular diffusion, which is several orders of magnitude smaller than the other terms and can be neglected [Yi *et al.*, 2000; Stull, 1988]. The horizontal turbulent flux divergence can also be taken out of equation (4), if the following conditions are met: presence of a fully developed convective boundary layer and a relatively homogeneous land surface [Yi *et al.*, 2000; Casso-Torralba *et al.*, 2008]. In that case the spatial scale of the horizontal flux divergence is much larger than the depth of the boundary layer and, therefore, the horizontal flux divergence is expected to be much smaller than the vertical turbulent flux divergence [Davis, 1992; Yi *et al.*, 2000]. Considering the relatively homogeneous surroundings of the measurement site and by selecting data under fair weather conditions, which will be explained later on, this is a reasonable assumption. After applying all the above mentioned simplifications we arrive at [Casso-Torralba *et al.*, 2008]:

$$\frac{\partial \bar{c}}{\partial t} + \bar{u} \frac{\partial \bar{c}}{\partial x} + \bar{w} \frac{\partial \bar{c}}{\partial z} + \frac{\partial \overline{w'c'}}{\partial z} = 0 \quad (5)$$

The net ecosystem exchange (*NEE*) of a scalar is defined as [Yi *et al.*, 2000]:

$$NEE \equiv \int_0^{Z_r} \bar{s}_c dz + (\overline{w'c'})_{z=0} \quad (6)$$

Here the second term on the right-hand side is the vertical turbulent flux at ground level. The first term on the right-hand side accounts for all sources and sinks ( $s_r$ ) of the scalar, vertically integrated between the surface and a certain reference height ( $Z_r$ ) above the ground. By combining this definition with equation (5) the following expression for  $NEE$  is obtained [Yi *et al.*, 2000; Casso-Torralba *et al.*, 2008]:

$$NEE_{Z_r} = \int_0^{Z_r} \frac{\partial \bar{c}}{\partial t} dz + (\overline{w'c'})_{Z_r} + \int_0^{Z_r} \left( \bar{u} \frac{\partial \bar{c}}{\partial x} + \bar{w} \frac{\partial \bar{c}}{\partial z} \right) dz \quad (7a)$$

$$NEE_{Z_r} = F_{ST} + F_{EC} + F_{AD} \quad (7b)$$

$NEE$ , using a certain observational level ( $Z_r$ ) above the ground, is now defined by the summation of the storage flux ( $F_{ST}$ ) below  $Z_r$ , the vertical turbulent flux ( $F_{EC}$ ) at  $Z_r$ , and the total advective flux ( $F_{AD}$ ) between the land surface and  $Z_r$ . The total advective flux includes a horizontal and a vertical component as can be seen in equation (7a). Since, at Cabauw, no sources or sinks for  $CO_2$  are present above ground level the difference between  $NEE$  using two different reference levels ( $z_1$  and  $z_2$ ) must be zero:

$$NEE_{z_1} - NEE_{z_2} = 0 \quad (8)$$

Next, using equation (7a) and equation (8), an expression is formulated which describes the total advective flux of  $CO_2$  between reference levels  $z_1$  and  $z_2$  [Casso-Torralba *et al.*, 2008]:

$$\int_{z_1}^{z_2} \left( \bar{u} \frac{\partial \bar{c}}{\partial x} + \bar{w} \frac{\partial \bar{c}}{\partial z} \right) dz = - \int_{z_1}^{z_2} \frac{\partial \bar{c}}{\partial t} dz + (\overline{w'c'})_{z_1} - (\overline{w'c'})_{z_2} = \Delta F_{AD} \quad (9)$$

Convective conditions allow for rewriting equation (9), because strong vertical mixing will cause the temporal evolution of  $c$  to be nearly independent of height. This assumption yields [Casso-Torralba *et al.*, 2008]:

$$\Delta F_{AD} = \int_{z_1}^{z_2} \left( \bar{u} \frac{\partial \bar{c}}{\partial x} + \bar{w} \frac{\partial \bar{c}}{\partial z} \right) dz = - \frac{\partial \bar{c}}{\partial t} \Delta z_{1,2} + (\overline{w'c'})_{z_1} - (\overline{w'c'})_{z_2} \quad (10a)$$

$$\Delta F_{AD} = -\Delta F_{ST} + F_{EC_1} - F_{EC_2} \quad (10b)$$

$$\Delta F_{AD} = -\Delta NEE_0 = NEE_{0(1)} - NEE_{0(2)} \Rightarrow \Delta NEE \quad (10c)$$

Equation (10c) is the final expression in order to quantify  $CO_2$  advection, where  $\Delta NEE$  denotes its measure, and which will be used throughout this report. It represents the total advective flux between two reference

heights, and is equal to the difference in  $NEE_o$  between two reference levels (lower level minus upper level), thus assuming  $NEE$  is simply the summation of  $F_{ST}$  and  $F_{EC}$  (see: introduction).

## 2.3. MEASUREMENTS AND COMPUTATIONS

In this study  $CO_2$  advection ( $\Delta NEE$ ) is taken as the residual term from the scalar budget methodology described above in section 2.1. The other budget terms from equation (10b), i.e.  $F_{EC}$  and  $F_{ST}$ , are derived from measurements along the Cabauw mast.

### 2.3.1. VERTICAL TURBULENT FLUX (EDDY COVARIANCE FLUX) ( $F_{EC}$ )

The Cabauw mast is equipped with LICOR-7500 open-path  $CO_2$  analyzers at 5, 60, 100 and 180 m height to measure the turbulent vertical flux *in-situ* at these levels. These sensors sample the  $CO_2$  concentration ( $c$ ) and the vertical wind speed ( $w$ ) at 10 Hz. An eddy covariance technique is used to retrieve flux data points on 10-minute time intervals. This technique in principle is based on the following concept [Stull, 2000b]:

$$covar(w, c) = \frac{1}{N} \sum_{k=1}^N (w_k - \bar{w}) (c_k - \bar{c}) \quad (11a)$$

$$= \frac{1}{N} \sum_{k=1}^N (w_k') (c_k') \quad (11b)$$

$$= \overline{w'c'} = F_{EC} \quad (11c)$$

Equations (11a-c) show that the flux is taken as the covariance between the vertical wind speed and the  $CO_2$  concentration, which is indicative of the amount of common variation between the two variables [Stull, 2000b].  $N$  denotes the amount of samples of  $w$  and  $c$  within a 10-minute measurement interval. Averages are denoted by an overbar and prime values denote deviations from the averages; i.e. prime values are the turbulent parts of the quantities [Stull, 2000b]. With dimensions of  $[m\ s^{-1}]$  for  $w$  and  $[mg\ m^{-3}]$  for  $c$  the unit for the vertical turbulent flux consequently becomes  $[mg\ m^{-2}\ s^{-1}]$ . This unit is used for all

fluxes in this report. In this study flux data points based on 30-minute time intervals are used, which are obtained from averaging the original 10-minute files. Webb corrections are applied to the flux measurements to account for density fluctuation, due to changes in humidity and temperature [Webb *et al.*, 1980; details of actual corrections: *online documentation – Bosveld*, 2010]. Corrections for tilt between inlets and air flow are also performed; see: Bosveld – *online documentation* [2010]. The instrumentation is calibrated ones a year. As a consequence, the fluxes can be systematically erroneous by 3% during several consecutive months.

### 2.3.2. CONCENTRATION AND STORAGE FLUX ( $F_{ST}$ )

To determine storage fluxes the CO<sub>2</sub> mixing ratio (ppm) is measured along the mast at 20, 60, 120 and 200 m height using Siemens Ultramat 5 instruments, with a resolution of 0.1 ppm. Using Permapure dryers the air is dried at the inlets to a dewpoint 15 °C below that of the ambient air, followed by drying to a dewpoint of -50 °C. Mixing ratios relative to dry air are hereby obtained. To arrive at the desired unit for storage fluxes of [mg m<sup>-2</sup> s<sup>-1</sup>] mixing ratios are converted to concentrations expressed as [mg m<sup>-3</sup>]. Even though the terminology is not completely sound, CO<sub>2</sub> mixing ratio as [ppm] will be structurally referred to as 'concentration' in this report. Storage fluxes can be calculated from:

$$F_{ST} = \frac{\partial \bar{c}}{\partial t} \Delta z_{(0,r)} = \frac{\bar{c}_{(t+\Delta t)} - \bar{c}_{(t)}}{\Delta t} \Delta z_{(0,r)} \quad (12)$$

Here  $\langle c \rangle$  denotes the mean concentration profile below a reference level ( $Z_r$ ) and  $\Delta t$  indicates a measurement time interval, which again spans 30 minutes; equal to the  $F_{EC}$  data. The reference levels of the storage fluxes are equated to the upper 3 observational levels of the vertical turbulent fluxes (60, 100 and 180 m). Because no concentration measurements are available at heights of 100 and 180 m, the mean concentration profile for these levels is derived from interpolation between the measurements below and above those heights. Furthermore, all available measurements below the reference heights are used to calculate mean concentration profiles. With [mg m<sup>-3</sup>] for  $\langle c \rangle$  and [m] for  $\Delta z$  the storage flux in equation (12) is thus also expressed as [mg m<sup>-2</sup> s<sup>-1</sup>].

### 2.3.3. NET ECOSYSTEM EXCHANGE (NEE) AND ADVECTIVE FLUX ( $\Delta NEE$ )

Advective flux ( $\Delta NEE$ ) 30-minute data in this study is calculated using the previously described measurements, reference heights and equation (10c). Therefore,  $\Delta NEE$  is expressed as [ $\text{mg m}^{-2} \text{s}^{-1}$ ] and is given for two height intervals: 60-100 m and 100-180 m. Estimations of the net ecosystem exchange ( $\text{mg m}^{-2} \text{s}^{-1}$ ), also from the 60, 100 and 180 m level, are discussed in this report as well. These data are referred to as ' $NEE$ ', but are actually calculated as  $NEE_o$  as given in equation (2).

### 2.3.4. WIND DIRECTION AND SHORT WAVE DOWN RADIATION

In this investigation wind direction ( $^\circ$ ) and short wave down radiation ( $\text{W m}^{-2}$ ) 30-minute averaged measurements are used. Wind direction is measured along the Cabauw mast at 10, 20, 80, 140 and 200 m height, using KNMI wind vanes. These measurements have a resolution of  $1^\circ$  and an accuracy of  $3^\circ$ . Wind direction data at heights where no *in-situ* measurement is available are obtained using interpolation between levels. Incoming shortwave down radiation is measured just south of the tower at a height of 1.5 m, using a Kipp & Zn CM11 pyranometer. The error in these measurements can be a few [ $\text{W m}^{-2}$ ] due to long wave radiative cooling.

## 2.4. DATA SELECTION, FILTERING AND CLEANING

The question of advective contribution to  $NEE$  under convective conditions is of primary importance to this investigation, as explained in the introduction and in the description of the scalar budget methodology (section 2.2). Additionally, a convective boundary layer with an established mixed layer exceeding the mast height leads to a quasi-steady state [Casso-Torralba *et al.*, 2008]. This state is anticipated to support the accuracy of flux measurements. At the same time, we want to estimate advection under regionally sunny daytime conditions with significant net  $\text{CO}_2$  uptake. Regionally homogeneous sunlight conditions stimulate a fair judgement of advection estimations, when the advection is due to  $\text{CO}_2$  sources and sinks in the Cabauw surroundings. In order to sample data under the above mentioned conditions a set of 'fair weather' criteria is selected, which are assumed to be representative herein:

- 1) study period: April-September
- 2) time: 0900-1600 UTC
- 3) sun irradiance: [ $\langle \text{measured } SWD \rangle$ ] / [ $\langle \text{clear sky } SWD \rangle$ ] > 0.7
- 4)  $NEE$ : [ $\langle NEE_{60m} \rangle$ ] <  $-0.3 \text{ mg m}^{-2} \text{ s}^{-1}$

The summer half year (criterion 1) is likely to be dominated by convective conditions with significant net  $\text{CO}_2$  uptake (criterion 4) during daytime. For criterion (4) the  $NEE$  estimation from a measurement height of 60 m is used. Between 0900 and 1600 UTC (criterion 2) the  $\text{CO}_2$  concentration was observed to be vertically near-homogeneous (see: section 3.1.1), contributing to the above mentioned quasi-stationary situation. During this daytime period one can generally anticipate to have convective mixing conditions. Finally, 'fair weather data' are sampled using criterion (3), where the measured short wave down ( $SWD$ ) radiation at Cabauw site must be at least 70% of the potential irradiance from the sun under a clear sky. It is hereby assumed that the sunny conditions also apply for the Cabauw surroundings. These criteria are generally applied to assess the relevance of  $\text{CO}_2$  advection and  $NEE$ . However,  $NEE$  and  $\Delta NEE$  data are also partly presented here for conditions that do not meet the criteria, if these serve to describe general patterns and processes (e.g. section 3.1). Fair weather selection is also referred to as 'standard selection' throughout this report.

Wind induced wake turbulence coming off the Cabauw mast itself is anticipated to perturb the eddy covariance measurements on the leeward side. The booms supporting the eddy covariance instruments are situated to the south-east ( $130^\circ$ ). For these reasons, all flux data with a mean wind direction - within the same 30-minute measurement interval - of  $310^\circ \pm 30^\circ$  are filtered out of the results.

Visual inspection of the eddy covariance flux data is performed for the entire period of study. This is done mainly because rain and high relative humidity are known to influence the instruments, leading to faulty measurements. Suspect data point are removed manually, and 'cleaned' data are stored in new 10-minute files, which are used to obtain the 30-minute data points for this study. All 30-minute concentration files are also visually inspected in the same way, where unlikely spikes are deleted from the data set and 'cleaned' data are obtained.

## 2.5. FOOTPRINTS AND CO<sub>2</sub> SOURCES/SINKS

A CO<sub>2</sub> turbulent flux measurement is mostly intended to reflect the exchange of the underlying surface with the atmosphere. In the ideal case of a perfectly homogeneous surface with infinite extent the exact measurement height is not important, because the surface flux at any location is by definition equal [Schmid, 2002]. Hence, trying to locate an area which influences a given turbulent flux receptor height would not be particularly interesting. This situation differs from inhomogeneous land surfaces, where the measured signal depends on the particular surface features of the area which most strongly influences the turbulent flux sensor. Therefore, it would be interesting to look for the so-called 'footprint' of a given receptor height in the surrounding landscape. Generally speaking, a footprint defines the spatial context of the measurement, providing a probable location and size. To illustrate this: a CO<sub>2</sub> particle emitted from a point between the sensor and the footprint does not reach the sensor at all. Particles reaching the sensor from farther away than the footprint have no correlation with the source [Schmid, 2002; Kljun *et al.*, 2004]. Within the footprint area, potential CO<sub>2</sub> sources and sinks could be designated, as done in this research.

A typical footprint function is a transfer function incorporating variables such as atmospheric stability, surface roughness and - obviously - the turbulent flux sensor height. Many analytical, numerical and stochastic model approaches have been developed over the years, which are based on concepts of e.g. internal boundary layers and effective fetch, and are applied in Lagrangian, Eulerian or e.g. Large Eddy Simulation (LES) frameworks. These approaches are extensively reviewed in the paper by Schmid [2002]. This investigation uses an approach adopted from a footprint parametrization by Kljun *et al.* [2004], with the objective to provide only footprint distance estimates (no footprint size or shape). These estimates give a probable distance from the Cabauw mast to the peak location of the footprint of a sensor. At the peak location the footprint function reaches a maximum for the given atmospheric conditions. Therefore, the sources or sinks for CO<sub>2</sub> at this location most strongly influence the flux at a given sensor height. Only those sensors used in  $\Delta NEE$  calculations are considered here. Below, a brief description is given of this methodology. For further details; see: Kljun *et al.* [2004].

Kljun *et al.* start with a scaling expression for a non-dimensional along-wind distance  $X_*$  based on the Buckingham  $\Pi$  Theorem [Stull, 1988] and 2  $\Pi$  groups, which reads as:

$$X_* = \left( \frac{\sigma_w}{u_*} \right)^{\alpha_1} \frac{x}{z_m} \quad (13)$$

In equation (13)  $\sigma_w$  is the standard deviation of vertical velocity fluctuations,  $u_*$  is the surface friction velocity,  $x$  is the distance from the sensor,  $z_m$  is the sensor height and  $\alpha_1$  is a free parameter. After their scaling exercise, model testing and parametrization they arrive at the following estimation for the distance to the peak location of a footprint,  $x_{max}$ :

$$x_{max} = X_{(*,max)} z_m \left( \frac{\sigma_w}{u_*} \right)^{-\alpha_1} \quad (14)$$

The first term on the right-hand side of equation (14) is their parametrization of equation (13) and is formulated as:

$$X_{(*,max)} = c - d \quad (15)$$

Here,  $c$  and  $d$  are fitting parameters. From their results and applying a typical regional value of the roughness length for Cabauw ( $z_0 = 0.1$  m) a value of  $\langle c - d \rangle = 15$  is obtained. Finally, with their finding of  $\alpha_1 = 0.8$ , and using a typical value of  $\langle \sigma_w / u_* \rangle = 1.25$  for neutral atmospheric stability conditions, we find the following estimations for the footprint peak location (Table I):

TABLE I  
Footprint peak location ( $x_{max}$ ) for vertical turbulent flux sensors used in  $\Delta NEE$  calculations.

Turbulent flux sensor height ( $z_m$ )	Footprint peak location ( $x_{max}$ )
60 m	750 m
100 m	1250 m
180 m	2250 m

## 2.6. MODELLING NET ECOSYSTEM EXCHANGE

In this study  $NEE$  data derived from measurements is compared to model based  $NEE$  output. A  $NEE$  model for  $CO_2$  is used, which closely resembles a model approach by *Jacobs et al.* [2007]. Some key aspects of this model are described below. *Jacobs et al.* tuned their model to eddy covariance flux measurements dating from 2002-2005. The model used in this study is optimized for the period of 2003-2006.

*Jacobs et al.* partition *NEE* into gross primary production (*GPP*) due to photosynthetic uptake and ecosystem respiration ( $R_e$ ):

$$NEE = GPP - R_e \quad (16)$$

Respiration, being strongly dependent on temperature, is approximated with the following equation:

$$R_e = R_{10} \exp\left[E_a \left(\frac{1}{10 - T_0} - \frac{1}{T - T_0}\right)\right] \quad (17)$$

In equation (17)  $R_{10}$  ( $\mu\text{mol m}^{-2} \text{s}^{-1}$ ) is the reference respiration rate at a temperature of 10°C,  $T$  (°C) is temperature and  $E_a$  (K) is the ecosystem activation energy or sensitivity coefficient.  $T_0$  is the zero respiration temperature, below which respiration has completely stopped. Its value:  $T_0 = -46.02^\circ\text{C}$ . *Jacobs et al.* use a photosynthesis-light response analysis technique to determine *GPP*, and write:

$$GPP = \frac{\alpha R_{in} GPP_{max}}{\alpha R_{in} + GPP_{max}} \quad (18)$$

Here,  $R_{in}$  ( $\text{W m}^{-2}$ ) is the incoming short wave radiation,  $\alpha$  ( $\mu\text{mol J}^{-1}$ ) is their light conversion factor, and  $GPP_{max}$  ( $\mu\text{mol m}^{-2} \text{s}^{-1}$ ) is the maximum gross assimilation rate. Equation (16) shows that their sign convention for *NEE* is reversed compared to the one used in this study. This is corrected and [ $\mu\text{mol}$ ]  $\text{CO}_2$  is converted to [mg]. In *Jacobs et al.* [2007] the temperature response was found from the data-set by optimization for various temperature classes. Here, we optimized the model in one go by using a functional form for the temperature response. For details, see: *Bosveld – online documentation* [2010].



## **3. RESULTS**

### **3.1. DIURNAL CYCLE OF CO<sub>2</sub> CONCENTRATIONS AND FLUXES**

The vertical distribution and temporal concentration evolution of CO<sub>2</sub> near the surface can be quite variable as many processes act on them. Atmospheric boundary layer dynamics, soil and vegetation processes and external forcings such as sunlight irradiance mainly determine this CO<sub>2</sub> budget. An additional contribution to the local budget can come from advection. In the discussion below seasonal variability of concentrations and vertical transport are scrutinized for Cabauw during the period of study. Because of high daily variability this is done by means of monthly averaged diurnal cycles.

#### **3.1.1. CONCENTRATION**

Here we present data for four months, i.e. December, April, July and August, to illustrate some typical seasonal concentration features. Figure 2 shows the average diurnal concentration cycle during December 2007 at 4 measurement heights and represents a typical winter day situation. Concentrations are relatively constant and high throughout the diurnal cycle, when compared to the current global mean tropospheric value of approximately 390 ppm [IPCC, 2007]. Results for December indicate a range of mean values of 398-417 ppm between 20 and 200 m height with the highest concentrations near the surface. Since daytime CO<sub>2</sub> uptake is weak and convective mixing plays a minor role during winter a significant vertical concentration gradient is typically maintained throughout a diurnal cycle. Winter time overall is dominated by respiration and is therefore characterized by relatively high concentrations. At the 20 m height a drop of about 10 ppm can be seen during daytime resulting from temporarily net assimilation and potentially some turbulent mixing with lower concentrations at higher levels. The concentration evolution around the same time of the 60 m and 120 m levels also suggests some vertical - yet weak - mixing.

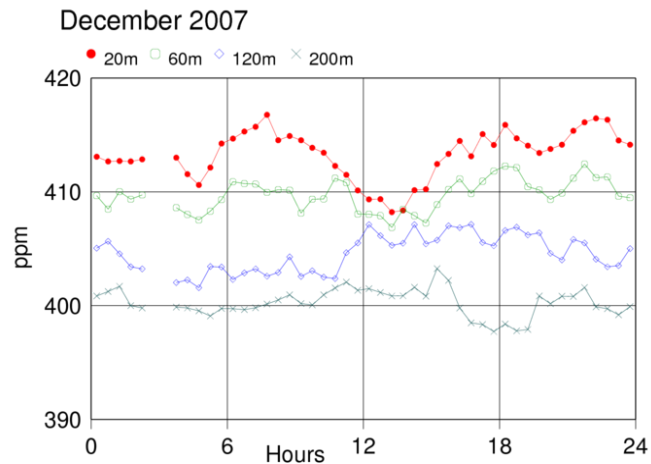


Figure 2. Monthly averaged diurnal cycle (UTC) of the concentration (ppm) at 4 measurement levels during December 2007. Measurement heights are denoted in the upper left corner.

During spring and summertime the typical situation is distinctly different as can be seen in the 3 figures below (Fig. 3-5) showing the average diurnal concentration cycle during April, July and August. CO<sub>2</sub> assimilation dominates during this part of the year leading to relatively low concentrations during the day. During daytime convection causes strong mixing resulting in a minor vertical concentration gradient along the tower. Moreover, the sign of this gradient is positive in the vertical. So, minimum concentrations are found closest to the ground, indicating the presence of a surface sink for CO<sub>2</sub>. The situation is thus reversed compared to December during these hours. However, it should be appreciated that this gradient is very small compared to December, or to spring and summer nights, and most pronounced close to the ground where CO<sub>2</sub> is assimilated.

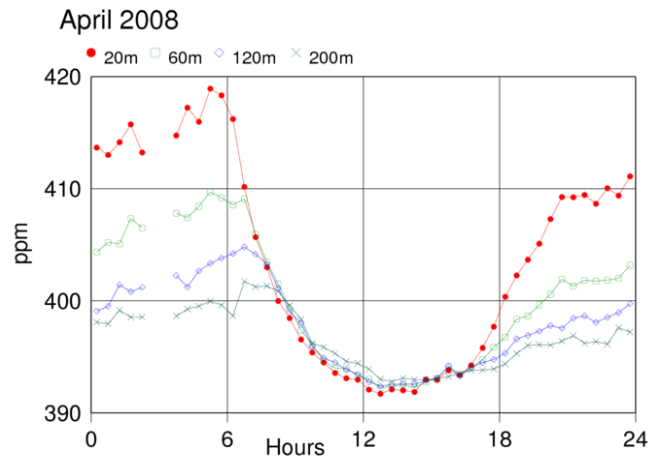


Figure 3. Monthly averaged diurnal cycle (UTC) of the concentration (ppm) at 4 measurement levels during April 2008. Measurement heights are denoted in the upper left corner.

At night, when a stable boundary layer forms and turbulent mixing is weak, CO<sub>2</sub> accumulates near the surface. This is mainly due to local soil and vegetation respiration processes, but advective contribution from surrounding anthropogenic or biogenic sources cannot be excluded [Werner *et al.*, 2004]. All this leads to a significant vertical concentration gradient, which can be observed in all 3 figures for April, July and August. Night time CO<sub>2</sub> levels increase at all 4 measurement heights suggesting vertical transport from the ground up to at least 200 m. Near the end of the day, when the boundary layer starts to develop from convective and well-mixed to stable and weakly-mixed, the concentration initially increases much faster near the ground, causing an increasing concentration gradient. Late at night the concentration typically increases at a similar rate at all 4 measurement heights. Accumulation ceases after sunrise when conditions change to a net uptake of CO<sub>2</sub> at ground level and a convective boundary layer develops. From Figures 3-5 it can be observed that the mixed layer grows up to 200 m height during roughly 2 morning hours and a near homogeneous vertical distribution is established. This phase will hereafter be referred to as the morning transition.

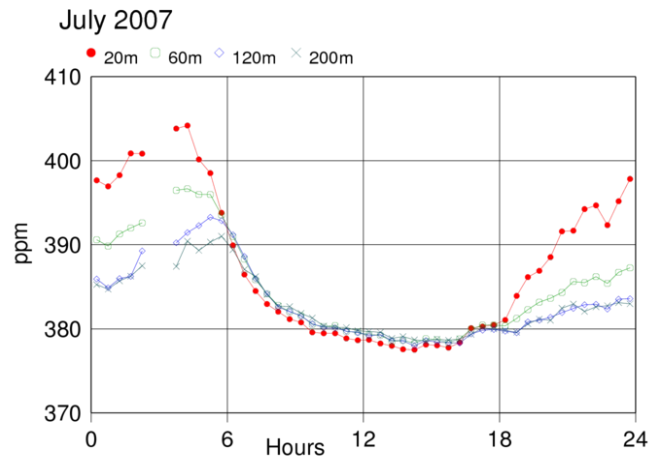


Figure 4. Monthly averaged diurnal cycle (UTC) of the concentration (ppm) at 4 measurement levels during July 2007. Measurement heights are denoted in the upper left corner.

The maximum concentration at 20 m, being reached at the threshold between nighttime accumulation and morning transition, differs between months. However, the results for July 2007-June 2008 do not indicate an obvious seasonal trend. Monthly averaged values range from 403 to 420 ppm, but are relatively constant between seasons. The minimum daytime concentration did show a pattern with the highest concentrations in December followed by a gradual 8-month decline reaching a mean lower bound of 376 ppm in August. The mean daytime minimum in April was 392 ppm and 378 ppm in July. After August the daytime minimum increases relatively fast, since it takes only 4 autumn months to reach the December peak. The nighttime concentration higher up, e.g. at 200 m, is more closely coupled to the daytime minimum concentration, due to weak vertical mixing at night. Hence, nighttime concentrations at 200 m reach a minimum during August as well. During April the pre-morning transition concentration at 200 m is approximately 400 ppm, 390 ppm during July and 385 ppm during August. Since the maximum nighttime concentration at 20 m is relatively constant throughout the seasons the nocturnal vertical concentration gradient peaks during August. Consequently, the largest night versus day concentration difference near the surface typically occurs during August as well. At 20 m height this difference averaged over August is 40 ppm, whereas it is only 10 ppm averaged over December, indicative of the end-of-summer versus winter conditions.

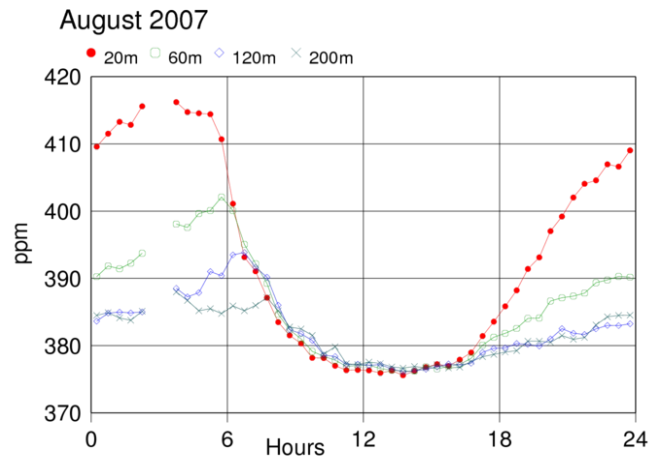


Figure 5. Monthly averaged diurnal cycle (UTC) of the concentration (ppm) at 4 measurement levels during August 2007. Measurement heights are denoted in the upper left corner.

Another seasonal aspect is near-homogeneous mixing duration. Obviously, the convective and therefore well-mixed part of the day is directly linked to the available daylight time. Therefore, the duration of daytime mixing at the Cabauw site is anticipated to peak in June or July. In this study period July shows the longest mean mixing duration of approximately 11 hours out of the mean 24 hour period. August and April are well-mixed up to 200 m during approximately 8/24 hours. January and February for instance (results not given here) showed a mean mixing duration of about 3 hours, whereas the averaged diurnal cycle during December shows no well-mixed period at all.

In summary, the CO<sub>2</sub> concentrations in the lower 200 m at Cabauw are quite variable, both in time and with height. Two important cycles were distinguished here: a diurnal and an annual one, where concentrations are relatively high at night and during wintertime. During the day and during summertime the concentrations are relatively low. At night there is typically strong accumulation of CO<sub>2</sub> near the surface, whereas convective mixing leads to a near-uniform concentration profile during the day.

### 3.1.2. FLUXES

Vertical CO<sub>2</sub> transport at Cabauw in terms of fluxes is discussed in the following section. These results show the vertical turbulent flux or eddy covariance flux (F<sub>ec</sub>), the storage flux (F<sub>st</sub>) and the net ecosystem

exchange (NEE). Again, a selection of 4 characteristic monthly averaged diurnal cycles serves to highlight some typical features. Note: a positive vertical turbulent flux implies upward transport. A negative one implies downward transport. A positive storage flux means that CO<sub>2</sub> has accumulated beneath the mentioned observational level in that measurement interval. Negative storage fluxes thus indicate a depletion of CO<sub>2</sub>.

The mean diurnal cycle of the above mentioned fluxes during August 2007 is given below in Figure 6. This month was selected because it nicely demonstrates a typical summer's day flux pattern, which is associated with significant net daytime CO<sub>2</sub> uptake, relatively high respiration rates at night and convective daytime conditions. Additionally, August has a seasonal significance, because of the annual daytime concentration minimum already stated in section 3.1.1. At night during this month wind induced turbulence was sufficient to measure vertical turbulent flux.

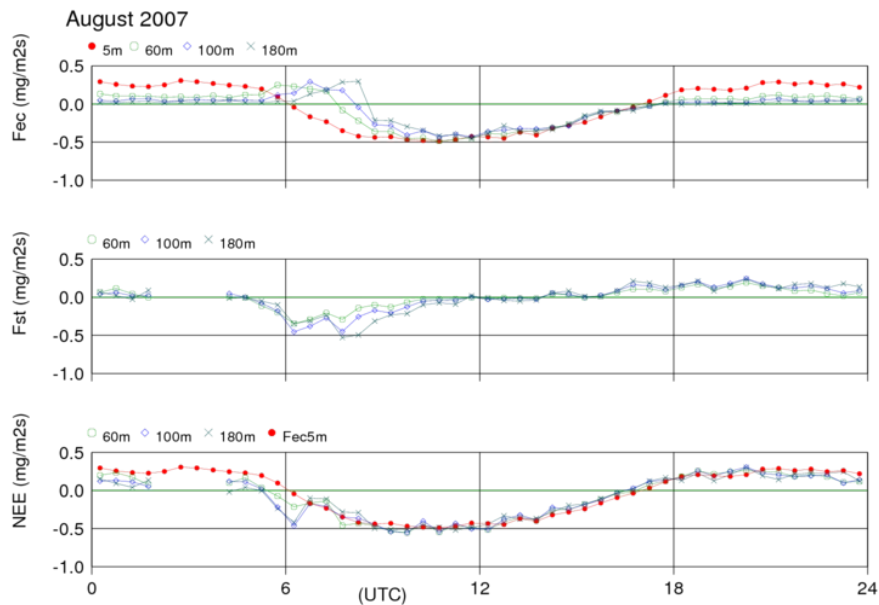


Figure 6. Monthly averaged diurnal cycle (UTC) of vertical turbulent flux (Fec), storage flux (Fst) and net ecosystem exchange (NEE) for August 2007. Data points are mean values per 30-minute time interval. All flux data in  $\text{mg m}^{-2} \text{s}^{-1}$ . Measurement heights are denoted in the upper left corner of a plot. Fec at 5 m height is also plotted in the lower panel.

At 5 m height the turbulent flux was  $\sim 0.2\text{-}0.3 \text{ mg m}^{-2} \text{ s}^{-1}$ , whereas at 60, 100 and 180 m the measured fluxes were much smaller with positive values of  $\sim 0\text{-}0.1 \text{ mg m}^{-2} \text{ s}^{-1}$ . During the first part of the night the

divergence of the vertical turbulent flux explains the positive storage flux ( $\sim 0.2 \text{ mg m}^{-2} \text{ s}^{-1}$ ) below each reference level reasonably well. The storage fluxes are also consistent with the observed increase in concentrations from the previous section and thus accurately reflect the process of nighttime accumulation. Around 0300 UTC there are no storage or NEE data because of insufficient concentration measurements. Despite this, Figure 6 does indicate that late at night the storage fluxes become smaller at all levels. Although this corresponds with the nocturnal concentration time lapse given in section 3.1.1, the turbulent flux divergence is similar to the early night and thus cannot explain this change. The NEE is positive throughout the night and initially closely follows the storage flux, because only the upper 3 turbulent flux measurements, showing low values, are used in estimating NEE. Consequently, the nighttime NEE is around  $0.2 \text{ mg m}^{-2} \text{ s}^{-1}$  with an upper bound of  $0.3 \text{ mg m}^{-2} \text{ s}^{-1}$  during the first part of the night. Late at night the contribution from the turbulent flux becomes more important when the storage decreases and NEE estimations show greater variability. NEE then ranges between 0 and  $0.2 \text{ mg m}^{-2} \text{ s}^{-1}$  depending on reference level. After sunrise  $\text{CO}_2$  respiration is soon surpassed by assimilation and the NEE becomes negative during morning hours. This is also clearly shown by the 5 m turbulent flux, which changes from 0.2 to  $-0.5 \text{ mg m}^{-2} \text{ s}^{-1}$ . During this morning transition a convective boundary layer develops resulting in efficient mixing and strong gradients in the turbulent flux profile emerge. Notice that this gradient is reversed compared to the night and progressively affects higher measurement levels as the boundary layer grows along the tower.  $\text{CO}_2$  which was accumulated at night is vented to higher levels while  $\text{CO}_2$  near the surface is taken up by the ecosystem. Meanwhile, entrainment at the top of the growing boundary layer transports lower  $\text{CO}_2$  content air from the residual layer downwards potentially contributing to the positive turbulent fluxes ( $\sim 0.3 \text{ mg m}^{-2} \text{ s}^{-1}$ ) measured at 60, 100 and 180 m. The consequent turbulent flux divergence causes a significant change in storage during morning hours with flux values down to  $-0.5 \text{ mg m}^{-2} \text{ s}^{-1}$ . After the morning transition all turbulent flux measurements change to negative values. Then  $\text{CO}_2$  is transported downwards along the entire mast. Also during this stage, the near-homogeneous concentration profile mentioned previously is established. During a few following morning hours concentrations (and therefore storage) continue to decrease, being vertically well-mixed, before stabilizing near the end of the morning. This can be recognized by a phase (around 0800 UTC) when the storage fluxes significantly differ from each other, being relatively low below 60 m and progressively higher below higher reference levels. This is due to the fact that during this phase the concentration below each level decreases at the same rate, and the subsequent storage flux follows from the mathematical product of that rate and the reference height. During the remainder of the morning hours the divergence of the turbulent flux typically diminishes. As the turbulent flux divergence decreases, so does the storage flux, which approaches 0 near the end of the morning hours, continuing as such during the afternoon. Entrainment potentially plays a role during the afternoon as well. As the mixed layer is being depleted from  $\text{CO}_2$  due to uptake at the surface, relatively  $\text{CO}_2$  rich air from the free troposphere - entrained at the top of the boundary layer - can partly compensate the loss and contribute to the negative

turbulent flux measured. The NEE is negative from the early morning until the end of the afternoon with most net uptake before 1200 UTC. The maximum net uptake rate is about  $-0.5 \text{ mg m}^{-2} \text{ s}^{-1}$  and becomes smaller during the afternoon, before reaching 0 when the evening starts. Towards the beginning of the evening respiration rates exceed assimilation and storage fluxes, turbulent fluxes and NEE change to positive values accordingly completing the diurnal cycle.

The averaged diurnal cycle of fluxes during May, given below in Figure 7, essentially shows a pattern similar to August and during roughly the same portion of the 24 hour period. This implies: nighttime accumulation reflected by positive turbulent fluxes, positive storage fluxes and positive NEE; a morning transition showing negative turbulent flux near the surface, positive higher up along with relatively strong negative storage flux; and negative NEE throughout the day. Yet, a few anomalies can be observed. At night the turbulent flux at 60 m is high compared to August. Other measurement levels indicate similar positive values during these hours. The nighttime storage fluxes are slightly smaller at first, but persist during the late night followed by a likely artifact (negative dip due to data limitation). The venting process during the morning transition is not that strong compared to August, since it is accompanied by smaller positive turbulent fluxes and smaller changes in storage spanning roughly the same morning hours.

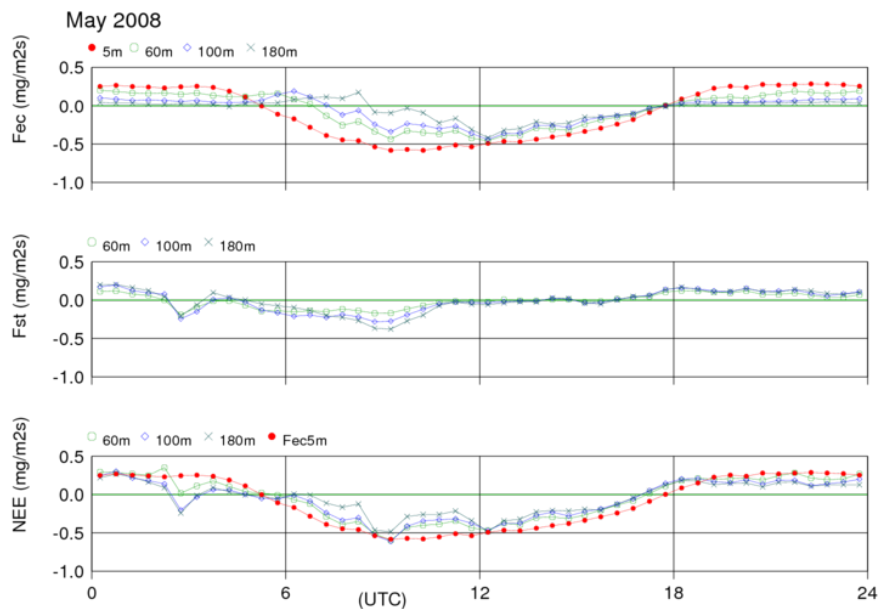


Figure 7. Monthly averaged diurnal cycle (UTC) of vertical turbulent flux (Fec), storage flux (Fst) and net ecosystem exchange (NEE) for May 2008. Data points are mean values per 30-minute time interval. All flux data in  $\text{mg m}^{-2} \text{ s}^{-1}$ . Measurement heights are denoted in the upper left corner of a plot. Fec at 5 m height is also plotted in the lower panel.

Most apparent of all differences though, is the persistent divergence of the turbulent flux during daytime. Where August shows a minor flux gradient from 5 to 180 m after the morning transition, the 3 upper levels lag behind the 5 m measurements. This feature is not supported by the storage flux data during the afternoon. Because this suggests a role for persistent advective contribution of the same sign, this month is specifically targeted in the section on advection (3.2). The NEE estimations of May are not very different from August with maximum net uptake of about  $-0.5 \text{ mg m}^{-2} \text{ s}^{-1}$  from the morning hours until the end of the day.

Results for July are shown below in Figure 8. Again, insufficient concentration measurements around 0300 UTC inhibit the storage flux and NEE data during this nighttime period. July was selected because of the extensive daytime period of net  $\text{CO}_2$  uptake. The day starts early in July as can be observed from the fluxes. At approximately 0400 UTC storage fluxes start to drop and the nocturnal turbulent flux divergence switches to the morning transition setting. Already as early as 0700 UTC the morning transition is over and all turbulent fluxes along the tower are negative. Storage reaches near 0 around 0800 UTC, which is about 2 hours earlier than either May or August. Moreover, the NEE estimations are negative, persistently showing great magnitude, from approximately 0500 UTC until 1800 UTC. NEE lower bounds are about  $-0.7 \text{ mg m}^{-2} \text{ s}^{-1}$ . Late at night the NEE estimations are relatively high, although being partly obscured by the data gap surrounding 0300 UTC. This follows from the turbulent fluxes at 60, 100 and 180 m, which are relatively high compared to other months.

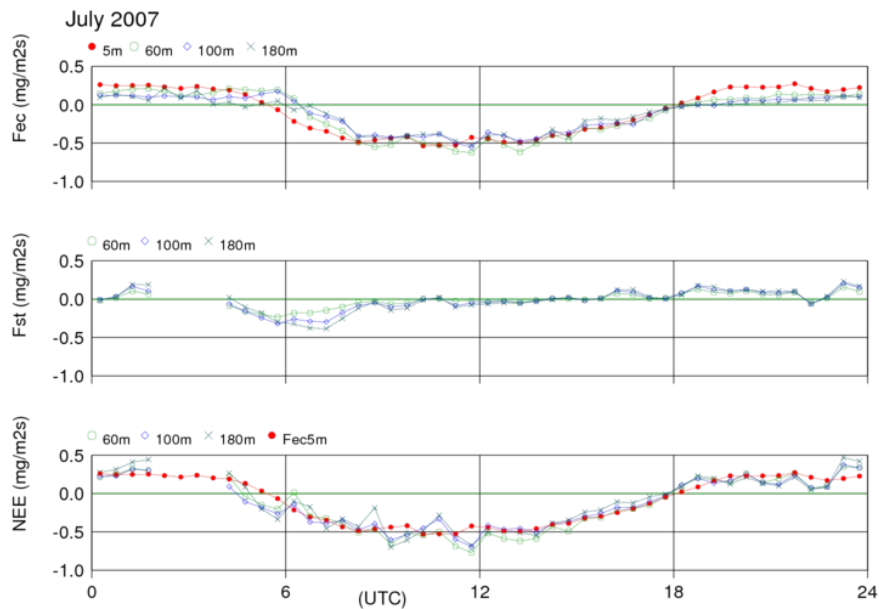


Figure 8. Monthly averaged diurnal cycle (UTC) of vertical turbulent flux ( $F_{ec}$ ), storage flux ( $F_{st}$ ) and net ecosystem exchange ( $NEE$ ) for July 2007. Data points are mean values per 30-minute time interval. All flux data in  $\text{mg m}^{-2} \text{ s}^{-1}$ . Measurement heights are denoted in the upper left corner of a plot.  $F_{ec}$  at 5m height is also plotted in the lower panel.

The month of December, given below in Figure 9, was chosen to illustrate fluxes during wintertime and to highlight the limitations of estimating the NEE from well above the ground during winter conditions. December nights are uneventful judging from the turbulent flux measurements, which indicate low positive values and minor divergence. This corresponds with the determination of fairly constant nocturnal concentrations in section 3.1.1. Storage fluxes and NEE estimations show an oscillating pattern of approximately  $-0.1$  to  $0.15 \text{ mg m}^{-2} \text{ s}^{-1}$  and  $-0.1$  to  $0.25 \text{ mg m}^{-2} \text{ s}^{-1}$ , respectively. Since net uptake of  $\text{CO}_2$  at night is highly unlikely, the negative NEE values appear unreliable. However, taken overall the NEE estimations indicate positive values at night. In contrast to the nighttime situation the daytime uptake might be underestimated by the NEE estimations. The 5 m turbulent flux measurements show that a small, but non-negligible, uptake takes place around 1200 UTC. This is not accurately represented by the NEE estimations. At the NEE reference levels the turbulent fluxes are positive because accumulated  $\text{CO}_2$  near the land surface is transported upwards. This coincides with storage fluxes being calculated using a minimum height of 20 m, above where the concentration is insufficiently affected by the sink at ground level due to weak mixing. I.e. storage changes are most significant closer to the surface. Therefore, the storage fluxes do not accurately represent reality, and the actual uptake is underestimated using these 3 reference levels along the mast. Consequently, the same argumentation applies for nighttime conditions when storage fluxes may inaccurately reflect  $\text{CO}_2$  build-up near the ground. During the mid-day period the turbulent flux at 5 m is about  $-0.1$  and  $< 0.25 \text{ mg m}^{-2} \text{ s}^{-1}$  at higher measurement levels. During other parts of the diurnal cycle it rarely exceeds  $0.1 \text{ mg m}^{-2} \text{ s}^{-1}$ .

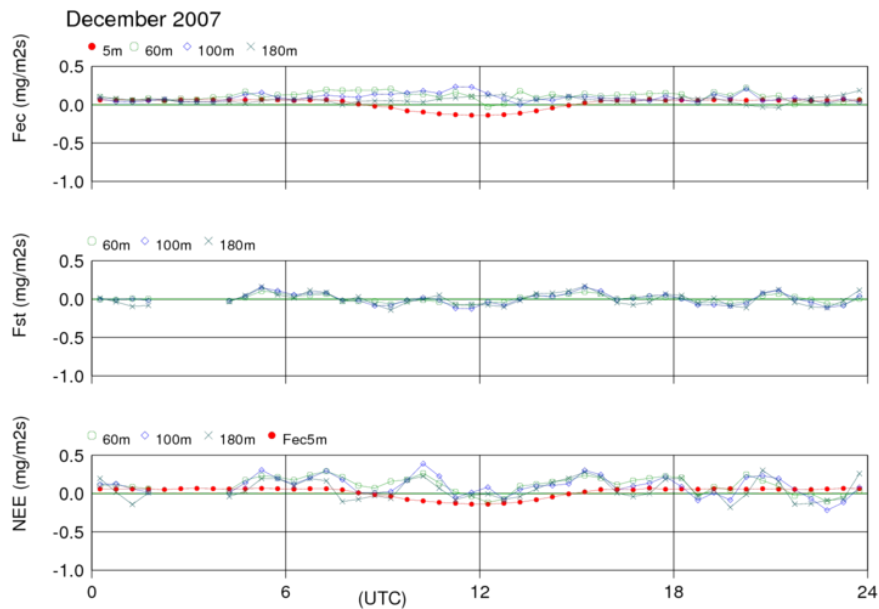


Figure 9. Monthly averaged diurnal cycle (UTC) of vertical turbulent flux ( $F_{ec}$ ), storage flux ( $F_{st}$ ) and net ecosystem exchange ( $NEE$ ) for December 2007. Data points are mean values per 30-minute time interval. All flux data in  $\text{mg m}^{-2} \text{ s}^{-1}$ . Measurement heights are denoted in the upper left corner of a plot.  $F_{ec}$  at 5 m height is also plotted in the lower panel.

In summary, the typical diurnal patterns of fluxes and concentrations (section 3.1.1) along the tower are generally in reasonable agreement. Nighttime accumulation of CO<sub>2</sub> near the surface is reflected by positive storage fluxes, as well as by a vertical gradient in the turbulent fluxes. A typical value for the monthly averaged nighttime surface flux into the atmosphere is about 0.3 mg m<sup>-2</sup> s<sup>-1</sup>. During the morning transition, with the onset of convective mixing and biological uptake at the surface, a strong vertical gradient in the turbulent fluxes emerges. Close to the surface CO<sub>2</sub> is then transported downwards and the accumulated CO<sub>2</sub> is 'moved' to higher levels as the morning progresses and the convective boundary layer grows. This translates into monthly averaged negative storage fluxes of approximately -0.3 mg m<sup>-2</sup> s<sup>-1</sup>. This phenomenon corresponds with the rapid decrease in concentrations shown in section 3.1.1. During daytime the storage is typically near-zero and the fluxes suggest a monthly averaged surface sink in the order of 0.5 mg m<sup>-2</sup> s<sup>-1</sup>.

### 3.1.3. NET ECOSYSTEM EXCHANGE

Two scatter plots are presented below in Figure 10 to briefly compare the NEE estimations using different reference levels. Data are for the 3-month period of April-June 2008 and were sampled using the standard selection criteria for time (0900-1600 UTC) and ratio of shortwave down radiation to clear sky radiation (>0.7). NEE 60m is plotted against NEE 100m and NEE 100m is plotted against NEE 180m. Spanning this time period the NEE mean values are very similar; approximately -0.4 to -0.45 mg m<sup>-2</sup> s<sup>-1</sup>. However, the lower reference level mean of each plot is slightly more negative. Figure 10 shows that this is the result of the departure from the diagonal at the more densely clustered part near the origin. At higher uptake rates this relation might have reversed in the case of NEE 60m vs. NEE 100m, but considering the amount of data points in that range this does not stand firmly. Deviation from the 1:1 lines indicates a noisier relation for NEE 100m vs. NEE 180m than for NEE 60m vs. NEE 100m. This is confirmed by the standard deviation relative to the regression line (*sigma y*), which is 0.155 in the left panel and 0.204 in the right panel of the figure (denoted by *SIGY* in the upper-left corner of a plot). Results for the late summer, i.e. July-September 2007 (not shown here), depict a similar situation with a slightly more negative mean NEE at the lower level (60m vs. 100m or 100m vs. 180m). Mean NEE values were slightly greater in magnitude; approximately -0.45 to -0.5 mg m<sup>-2</sup> s<sup>-1</sup>. This period yielded only about half of the amount of NEE data points relative to April-June and is not shown here.

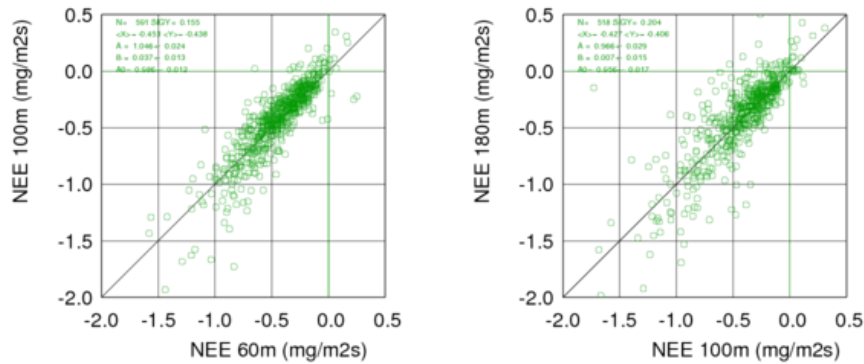


Figure 10. Scatter plots of all 30-minute NEE estimations ( $\text{mg m}^{-2} \text{s}^{-1}$ ) during April-June 2008 using standard selection criteria for time (9-16 UTC) and ratio shortwave down radiation/clear sky radiation ( $>0.7$ ). Left panel shows NEE 60m vs. NEE 100m. Right panel shows NEE 100m vs. NEE 180m.

A direct relationship exists between  $\text{CO}_2$  assimilation and sunlight irradiance, since photosynthesis is strongly light dependent. Therefore, the NEE estimations of this study are anticipated to point out some degree of correlation with sunlight intensity. To this end, measured short wave down radiation at Cabauw is plotted versus the NEE estimations at 3 reference levels. These results – for April-June 2008 - are given below in Figure 11, where standard sampling criteria were applied. Indeed, higher incoming short wave radiation intensity is typically associated with higher net uptake rates. Also is seen that higher reference levels lead to more spread in the data. Another feature, which is most apparent in the NEE 60m plot, is the NEE behavior at high irradiance. Up to about  $700 \text{ W m}^{-2}$  the relationship appears roughly linear, whereas at higher radiation intensity there are relatively low net uptake values. This could potentially be linked to temperature. As high sunlight irradiance is typically associated with high temperatures, the vegetation at Cabauw might react by closing stomata in order to reduce transpiration, consequently limiting the uptake of  $\text{CO}_2$ . Another suggestion is light saturation, which is a phenomenon described by *Jacobs et al.* [2007]. An increasingly noisier relationship at higher levels is likely due to the statistical nature of flux measurements. Higher up in the atmosphere less eddies pass by in a measurement time interval, hampering the statistical strength [Stull, 2000a].

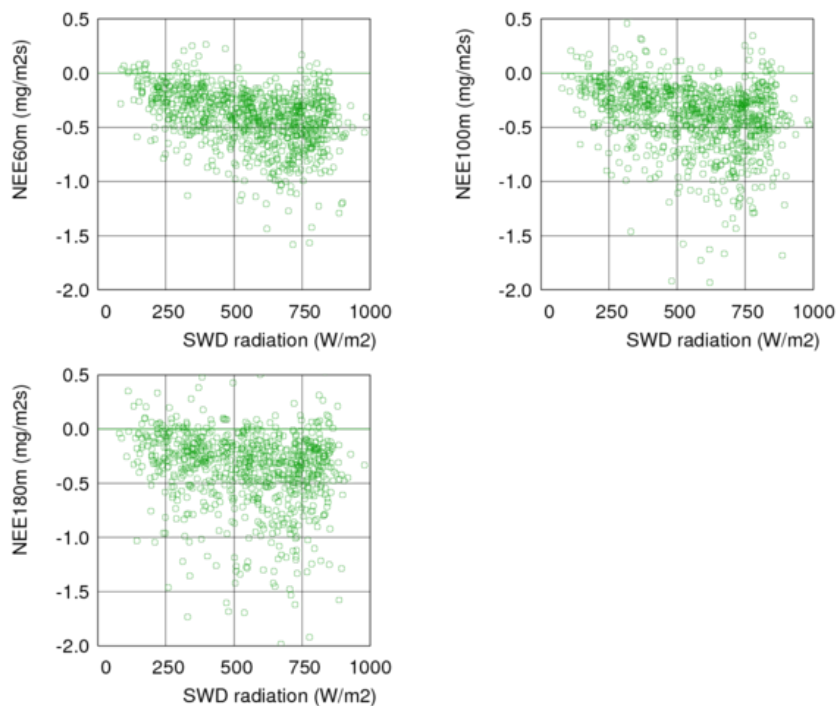


Figure 11. Scatter plots of all 30-minute NEE estimations ( $\text{mg m}^{-2} \text{s}^{-1}$ ) versus measured short wave down (SWD) radiation ( $\text{W m}^{-2}$ ) during April-June 2008 using standard selection criteria for time (9-16 UTC) and ratio shortwave down radiation/clear sky radiation ( $>0.7$ ). Upper left panel shows NEE 60m vs. radiation. Upper right panel shows NEE 100m vs. radiation. Lower panel shows NEE 180m vs. radiation.

NEE estimations have been compared to output from a respiration-assimilation model (see: method section 2.6). August 2007 is taken as an example. Figure 12 shows the averaged NEE diurnal cycle based on measurements, the NEE diurnal cycle produced by the model and the anomaly, being: [measurement NEE – model NEE]. The model produces a clean temporal pattern of nocturnal respiration and net assimilation during daytime. The flux at night is quite steady with values approximately  $0.2\text{-}0.25 \text{ mg m}^{-2} \text{ s}^{-1}$  and daytime net uptake reaches a maximum of about  $-0.4 \text{ mg m}^{-2} \text{ s}^{-1}$ . The measurement based NEE estimations are generally more erratic (not as smooth). In the August case the early night shows relatively low anomaly, but during the late night the  $\text{CO}_2$  release from the surface is low compared to the model. This is especially valid for the higher reference levels. Going into the morning transition net uptake rates are relatively high before a short period sets in where the NEE estimations and model data are in reasonable agreement. The following morning hours again indicate relatively high values for the net uptake relative to the model. Afterwards, during the afternoon, values become more consistent between model and

observations, except between 1500 and 1800 UTC; where the estimations suggest higher NEE than the model. Regarding the results from other months (without presenting plots): April and July, for instance, have similar anomalous behavior during the morning, afternoon and early night. However, during the late night the measurement based NEE values are more positive than the model output. Daytime during May showed significantly underestimated net uptake up to an anomaly of  $\sim 0.3 \text{ mg m}^{-2} \text{ s}^{-1}$ , spanning virtually the entire daylight period. The term 'underestimated' is used here because advection is - at least in part - causing this difference. This will be explained in the next section, which is solely on advection.

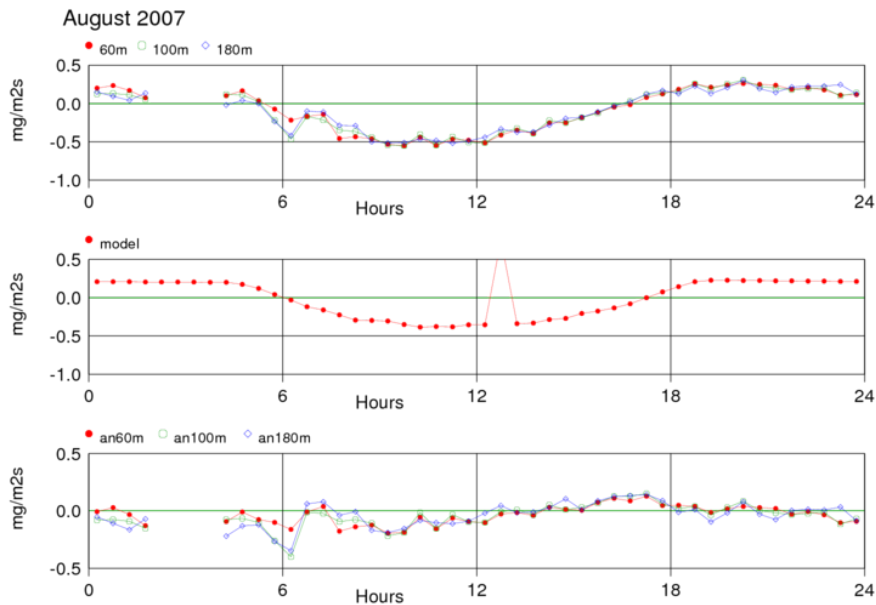


Figure 12. Comparison between NEE estimation based on measurements and on model output for August 2007. Upper panel gives the average diurnal cycle (UTC) using measurements (3 reference levels), middle panel gives model output and lower panel gives the anomaly (an) of the 3 reference levels. If applicable, reference levels are denoted in the upper left corner of a plot. All data in  $\text{mg m}^{-2} \text{ s}^{-1}$ .

In summary, a single mean value over several months for the NEE estimation at different levels is similar. These suggest a typical value for the daytime  $\text{CO}_2$  uptake of  $0.4$  or  $0.5 \text{ mg m}^{-2} \text{ s}^{-1}$ . But, the data from higher levels does become more variable and slightly less negative on average (less uptake). Compared to a NEE-model the highest observational level also showed the greatest anomaly. Increased variability with height can be caused by an increasing influence of advection or measurement issues. If advection is the cause for slightly less negative numbers at higher levels, this would suggest that advection of  $\text{CO}_2$  enriched air (slightly) dominates on average, when going higher up in the air.

## 3.2. ADVECTION

In this section CO<sub>2</sub> advection estimations at the Cabauw site are discussed. Calculated  $\Delta NEE$  values represent the advection term between reference levels on the basis of 30-minute time intervals. The sign convention is such that negative values suggest advection of CO<sub>2</sub> enriched air, whereas positive values suggest advection of relatively low CO<sub>2</sub> content air.

### 3.2.1. MONTHLY AND 3-MONTHLY AVERAGED DIURNAL CYCLES OF $\Delta NEE$

Figure 13 shows the diurnal cycle of  $\Delta NEE$  averaged over a 3 month period from April-June 2008. Both the 60-100 m and 100-180 m height estimations indicate persistent positive advective flux at night ( $\sim 0.05$  mg m<sup>-2</sup> s<sup>-1</sup>). This suggests that on average the measurement site is influenced by less enriched air from its surroundings during nighttime. The mean  $\Delta NEE$  signal for this time period becomes more erratic towards the early morning, starting as early as 0200 UTC for the 100-180 m calculation. Although the trend remains positive the error bars in Figure 13 indicate significant deviation from the mean. This suggest that CO<sub>2</sub> enriching advection also plays a role within this period, on time scales smaller than 3 months (days or e.g. individual months). Mean values range from -0.05 to 0.2 mg m<sup>-2</sup> s<sup>-1</sup>.

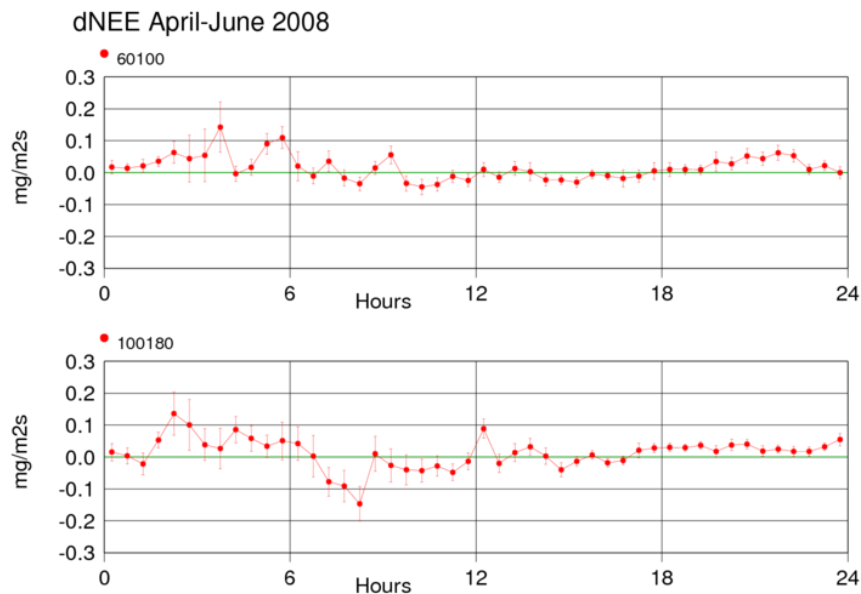


Figure 13. Average diurnal cycle (UTC) of  $\Delta NEE$  (mg m<sup>-2</sup> s<sup>-1</sup>) April-June 2008. Upper panel shows  $\Delta NEE$  between 60 and 100 m. Lower panel shows  $\Delta NEE$  between 100 and 180 m. Error bars display standard error in the mean per 30-minute time interval.

During these months the morning transition period is associated with significant negative advective flux between 100 and 180 m height reaching  $\sim -0.2 \text{ mg m}^{-2} \text{ s}^{-1}$ . Between 60 and 100 m height the advective contribution appears to be typically positive during the early morning transition, thereafter showing substantial fluctuations around 0. Daytime after the morning transition shows variable advective contribution averaged over this time period with some tendency towards negative values, being most pronounced between 60-100 m. Advection is in the order of  $\pm 0.05\text{-}0.1 \text{ mg m}^{-2} \text{ s}^{-1}$ . Figure 14 shows the  $\Delta\text{NEE}$  diurnal cycle for April-June 2008. These 30-minute data were retrieved using the selection on fair weather daytime periods. Essentially similar results are obtained using the fair weather selection, showing fluctuations around 0 with a weak trend of mean enriching advection. However, some data points in the 100-180 m calculation show increased variability, compared to those without fair weather selection, as indicated by the error bars in figure 14. This is due to a lower number of data points. Mean advective flux using this selection is approximately  $\pm 0.05\text{-}0.15 \text{ mg m}^{-2} \text{ s}^{-1}$  between the morning transition and nighttime.

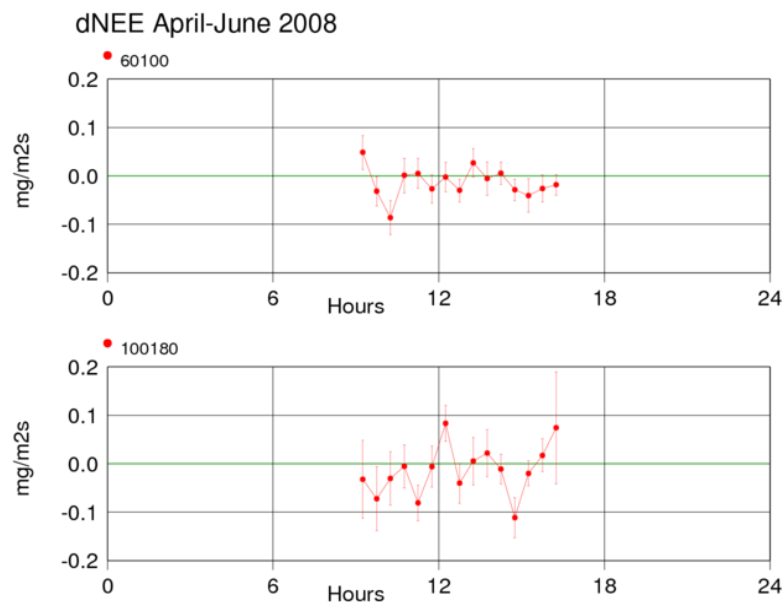


Figure 14. Average diurnal cycle (UTC) of  $\Delta\text{NEE}$  ( $\text{mg m}^{-2} \text{ s}^{-1}$ ) for April-June 2008 with selection criteria for time (9-16 UTC), NEE 60m ( $< -0.3 \text{ mg m}^{-2} \text{ s}^{-1}$ ) and ratio shortwave down radiation/clear sky radiation ( $> 0.7$ ). Upper panel shows  $\Delta\text{NEE}$  between 60 and 100 m. Lower panel shows  $\Delta\text{NEE}$  between 100 and 180m. Error bars display standard error in the mean per 30-minute time interval.

Results from the late summer under study are given in Figures 15 and 16. Firstly, the average  $\Delta\text{NEE}$  diurnal cycle without selection for July-September 2007 is shown, followed by the average diurnal cycle including the previously mentioned criteria for time, NEE and sunlight. Missing data around 0300 UTC are

due to insufficient concentration measurements during these months. An average trend of small but persistently positive values during nighttime, as observed in the April-June case, cannot be derived from these results. After the morning transition during daytime persistent negative flux between 60-100 m suggests CO<sub>2</sub> enriching advection is a dominant feature at this level during this period and these hours. The daytime behavior of mean  $\Delta NEE$  100-180 m is more erratic around 0, but shows some tendency towards  $\Delta NEE < 0$ . Except for the morning transition mean daytime advection estimations are in the order of  $-0.05$  to  $-0.1 \text{ mg m}^{-2} \text{ s}^{-1}$  between 60-100 m and  $-0.1$ - $0.05 \text{ mg m}^{-2} \text{ s}^{-1}$  between the 100 and 180 m level. Going into the morning transition at 60-100 m height a drastic positive shift in flux up to  $\sim 0.2 \text{ mg m}^{-2} \text{ s}^{-1}$  can be seen in Figure 15 preceding a sudden drop to  $\Delta NEE < 0$  during the next time interval. This event is followed by another rapid increase to positive values remaining so for about 1 hour in this 3-month average. Hereafter, the previously mentioned daytime pattern of enriching advection sets in. At 100-180 m height morning hours show a high variability concerning CO<sub>2</sub> advection showing standard errors in the mean well below and above 0. However, the calculated mean is typically negative during this period. The nighttime towards early morning positive peaks observed from April-June 2008 cannot be compared to July-September 2007 since data around 0300 UTC are not available from the latter period. Figure 16 shows  $\Delta NEE$  results using the mentioned selection criteria for July-September 2007. The sign of  $\Delta NEE$  60-100 m is also predominantly negative, but more variable than without the selection.  $\Delta NEE$  100-180 m is again highly variable showing similar peaks as in figure, but with greater magnitude. Advective flux is approximately  $-0.2$ - $0.1 \text{ mg m}^{-2} \text{ s}^{-1}$ .

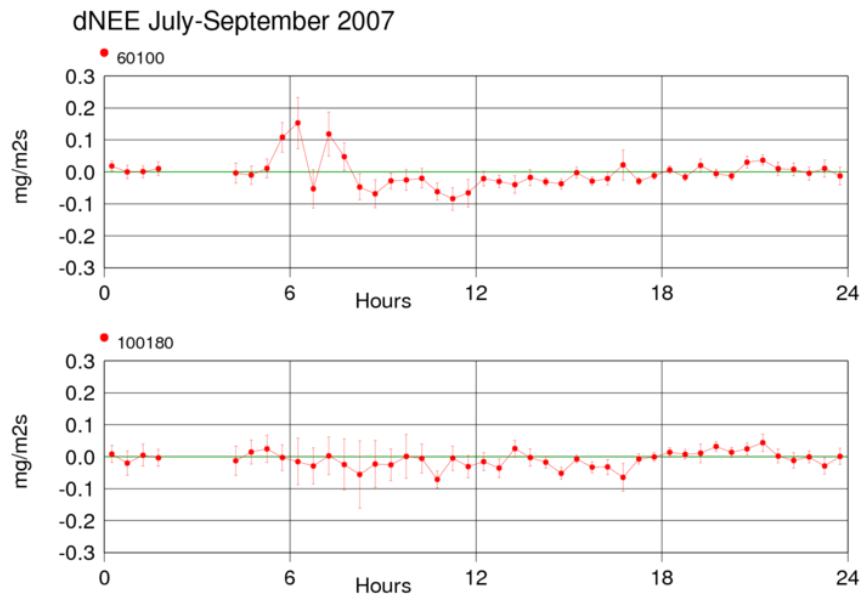


Figure 15. Average diurnal cycle (UTC) of  $\Delta NEE$  ( $\text{mg m}^{-2} \text{ s}^{-1}$ ) July-September 2007. Upper panel shows  $\Delta NEE$  between 60 and 100 m. Lower panel shows  $\Delta NEE$  between 100 and 180 m. Error bars display standard error in the mean per 30-minute time interval.

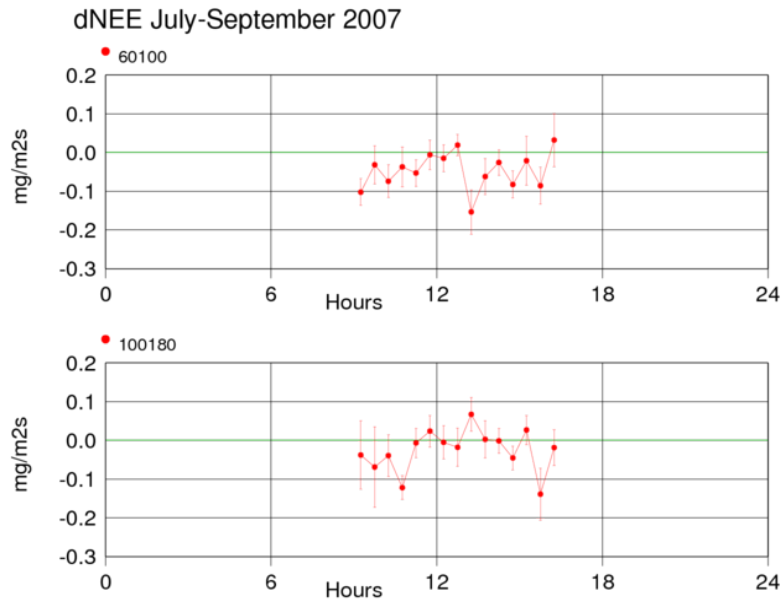


Figure 16. Average diurnal cycle (UTC) of  $\Delta NEE$  ( $\text{mg m}^{-2} \text{s}^{-1}$ ) for July-September 2007 with selection criteria for time (9-16 UTC),  $NEE_{60m}$  ( $< -0.3 \text{ mg m}^{-2} \text{ s}^{-1}$ ) and ratio shortwave down radiation/clear sky radiation ( $> 0.7$ ). Upper panel shows  $\Delta NEE$  between 60 and 100 m. Lower panel shows  $\Delta NEE$  between 100 and 180m. Error bars display standard error in the mean per 30-minute time interval.

In summary, diurnal cycles averaged over 3 months predominantly show a noisy signal of alternately depleting and enriching advection. But, during some hours of the diurnal cycles the signal is significant and persistent. The advective contribution to NEE is mainly in the order of 10-20%. It seems that at night depleting advection dominates. Especially during the late night and the morning hours the advection can be relatively strong, possibly contributing up to 40% of NEE. The advective contribution both under fair weather conditions and all-weather conditions appears to be similar.

Monthly averaged diurnal cycles of  $\Delta NEE$  are given below for May 2008, June 2008 and August 2007. These months were selected because of apparent reoccurring diurnal patterns in the monthly averages. Three figures per month respectively show the average diurnal cycle, the average diurnal cycle with the selection criteria and the diurnal cycle with selection using the median instead of the mean per 30-minute time interval.

A significant daytime trend of enriching advection is observable during May 2008 (Fig. 17-19). Especially between 100-180 m the mean advective flux associated with the morning transition is strong with

deviations below  $-0.2 \text{ mg m}^{-2} \text{ s}^{-1}$ . Late morning and early afternoon values fluctuate around  $-0.1 \text{ mg m}^{-2} \text{ s}^{-1}$ . The negative flux between 60-100 m is smaller throughout the day, but shows an obvious negative trend as well. Mean values are around  $-0.05 \text{ mg m}^{-2} \text{ s}^{-1}$ . At night advection at this level is typically positive ( $\sim 0.05\text{-}0.1 \text{ mg m}^{-2} \text{ s}^{-1}$ ) with some extreme peaks around 0300 UTC showing deviation up to  $0.3 \text{ mg m}^{-2} \text{ s}^{-1}$ . Also for the 100-180 m level a pattern of mean depleting advection can be observed at night. However, the signal becomes noisier late at night on to the early morning. Similar but less smooth results are obtained when applying the selection criteria in interval mean and median calculations. The 100-180 m level shows the highest enriching flux of around  $-0.1 \text{ mg m}^{-2} \text{ s}^{-1}$  with extremes of a about  $-0.2 \text{ mg m}^{-2} \text{ s}^{-1}$ . Between 60 and 100 m the range is  $\sim 0.05 \text{ mg m}^{-2} \text{ s}^{-1}$  with peaks down to  $-0.1 \text{ mg m}^{-2} \text{ s}^{-1}$ .

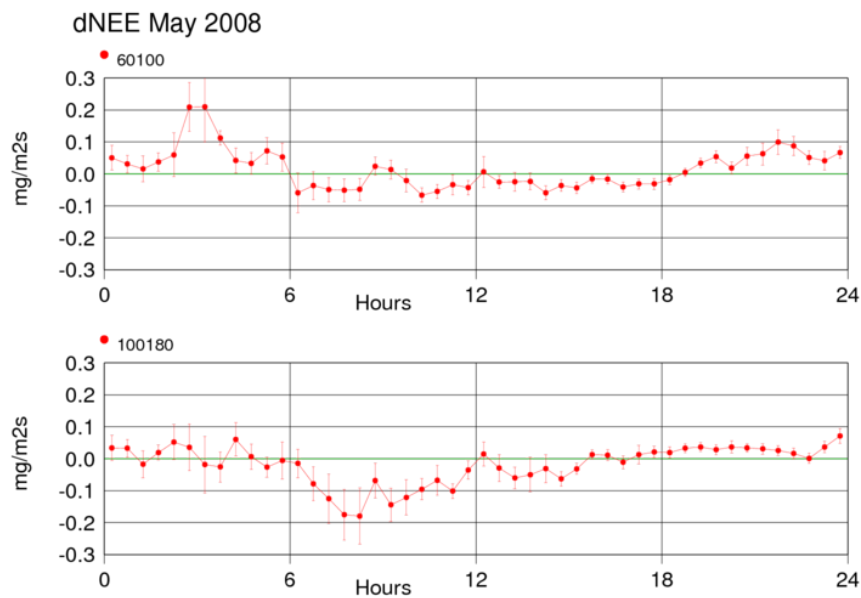


Figure 17. Average diurnal cycle (UTC) of  $\Delta NEE$  ( $\text{mg m}^{-2} \text{ s}^{-1}$ ) for May 2008. Upper panel shows  $\Delta NEE$  between 60 and 100 m. Lower panel shows  $\Delta NEE$  between 100 and 180 m. Error bars display standard error in the mean per 30-minute time interval.

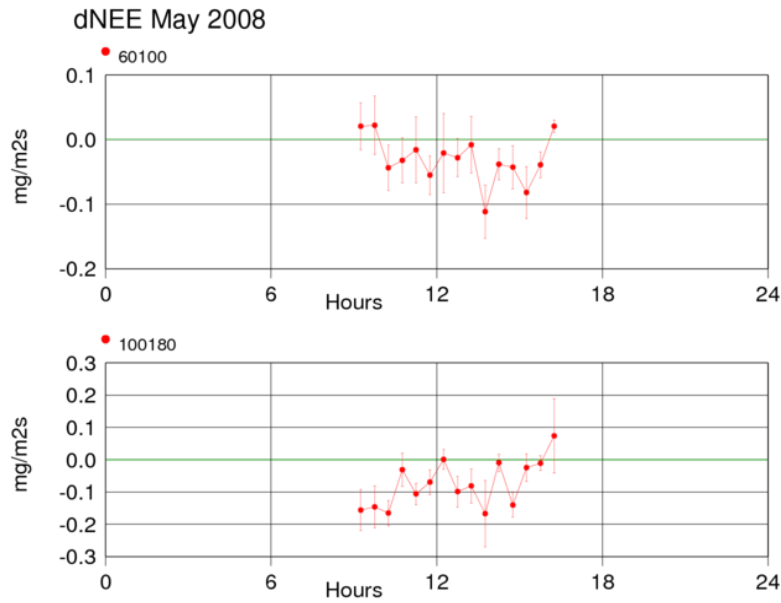


Figure 18. Average diurnal cycle (UTC) of  $\Delta NEE$  ( $\text{mg m}^{-2} \text{s}^{-1}$ ) for May 2008 with selection criteria for time (9-16 UTC), NEE 60m ( $< -0.3 \text{ mg m}^{-2} \text{ s}^{-1}$ ) and ratio shortwave down radiation/clear sky radiation ( $> 0.7$ ). Upper panel shows  $\Delta NEE$  between 60 and 100 m. Lower panel shows  $\Delta NEE$  between 100 and 180m. Error bars display standard error in the mean per 30-minute time interval.

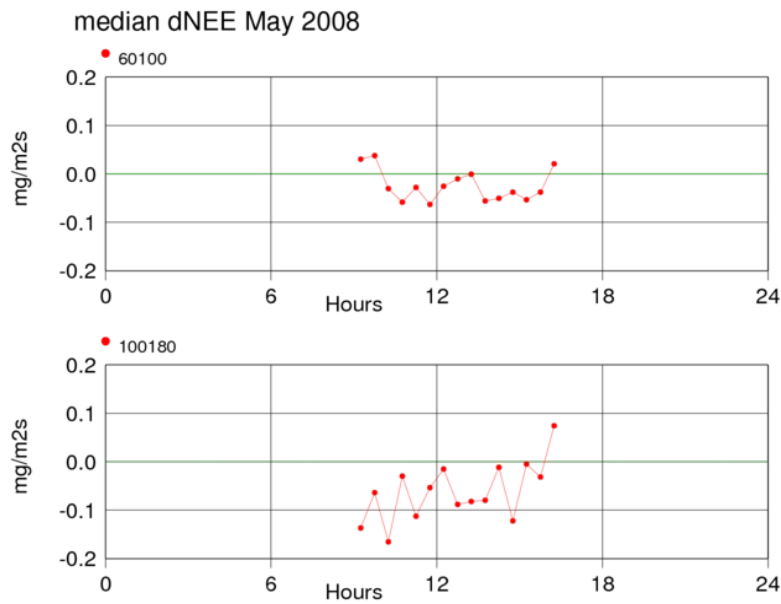


Figure 19. Diurnal cycle (UTC) of median values  $\Delta NEE$  ( $\text{mg m}^{-2} \text{ s}^{-1}$ ) for May 2008 with selection criteria for time (9-16 UTC), NEE 60m ( $< -0.3 \text{ mg m}^{-2} \text{ s}^{-1}$ ) and ratio shortwave down radiation/clear sky radiation ( $> 0.7$ ). Upper panel shows  $\Delta NEE$  between 60 and 100 m. Lower panel shows  $\Delta NEE$  between 100 and 180m.

Results for June 2008 (Fig. 20) indicate a period, roughly 1600-2200 UTC, with persistent positive advective flux ( $\sim 0-0.15 \text{ mg m}^{-2} \text{ s}^{-1}$ ) between the 60 and 100 m level. After this period negative values show up and variability increases throughout the average June night. At the same time the 100-180 m level shows an oscillating, yet slightly positive pattern, followed by highly positive flux ( $\sim 0.1-0.3 \text{ mg m}^{-2} \text{ s}^{-1}$ ) late at night and early morning. Shortly after sunrise when the boundary layer typically evolves from stable stratification to being convective and well-mixed a peak of depleting advection of approximately  $0.2-0.3 \text{ mg m}^{-2} \text{ s}^{-1}$  or higher occurs between 60 and 100 m. Also anticipated to be related to the morning transition, Figure 20 shows a significant drop to negative advective flux at the 100-180 m level lagging behind the event at the lower reference levels. This drop interrupts an otherwise predominantly positive trend of means during this time of day in June. No obvious pattern can be detected during the afternoon in the results using mean 30-minute interval values. This is valid for both the selection and non-selection data. However, applying the selection to yield median values leads to some tendency towards more enriching advection between 60 and 100 m and depleting advection between 100 and 180 m.

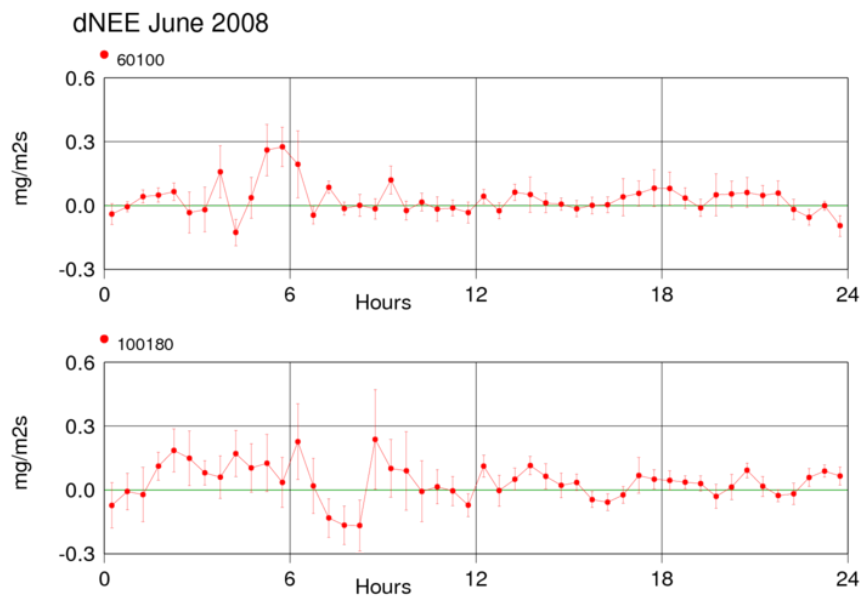


Figure 20. Average diurnal cycle (UTC) of  $\Delta NEE$  ( $\text{mg m}^{-2} \text{ s}^{-1}$ ) for June 2008. Upper panel shows  $\Delta NEE$  between 60 and 100 m. Lower panel shows  $\Delta NEE$  between 100 and 180 m. Error bars display standard error in the mean per 30-minute time interval.

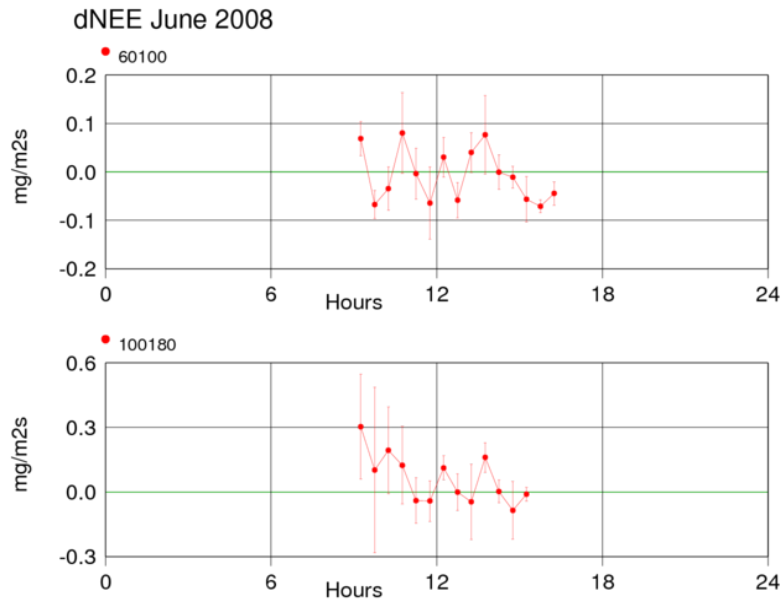


Figure 21. Average diurnal cycle (UTC) of  $\Delta NEE$  ( $\text{mg m}^{-2} \text{s}^{-1}$ ) for June 2008 with selection criteria for time (9-16 UTC), NEE 60m ( $< -0.3 \text{ mg m}^{-2} \text{ s}^{-1}$ ) and ratio shortwave down radiation/clear sky radiation ( $> 0.7$ ). Upper panel shows  $\Delta NEE$  between 60 and 100 m. Lower panel shows  $\Delta NEE$  between 100 and 180m. Error bars display standard error in the mean per 30-minute time interval.

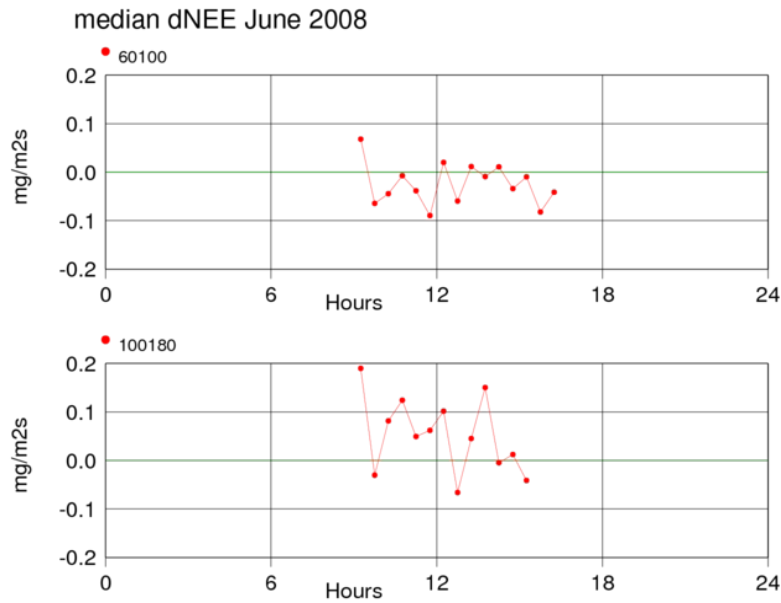


Figure 22. Diurnal cycle (UTC) of median values  $\Delta NEE$  ( $\text{mg m}^{-2} \text{s}^{-1}$ ) for June 2008 with selection criteria for time (9-16 UTC), NEE 60m ( $< -0.3 \text{ mg m}^{-2} \text{ s}^{-1}$ ) and ratio shortwave down radiation/clear sky radiation ( $> 0.7$ ). Upper panel shows  $\Delta NEE$  between 60 and 100 m. Lower panel shows  $\Delta NEE$  between 100 and 180m.

Average  $\Delta NEE$  results from August 2007 show a pattern similar to the previously discussed months during morning hours. Soon after sunrise significant advection of relatively low  $\text{CO}_2$  content air is observed at the lower reference levels. Mean values have an upper bound of about  $0.3 \text{ mg m}^{-2} \text{ s}^{-1}$ . This occurrence coincides with a trend of enriching advective flux at the higher measurement levels as seen in Figure 23. The latter daily trend in this month, however, does show a large spread surrounding the mean values. Calculated mean values are negative, but have a standard error in the mean of approximately  $\pm 0.1 \text{ mg m}^{-2} \text{ s}^{-1}$  and therefore weaken the trend. Due to insufficient concentration measurements  $\Delta NEE$  data around 0300 UTC is absent. However, adjacent data points suggest positive flux late at night on to the early morning between 100 and 180 m height. During other hours the average diurnal cycle without selection criteria does not provide convincing inclination towards either sign in flux. For the remainder of the averaged 24 hour period the mean influence by advection is in the order of  $\pm 0.05 \text{ mg m}^{-2} \text{ s}^{-1}$  between 60 and 100 m and  $\pm 0.1 \text{ mg m}^{-2} \text{ s}^{-1}$  for the upper reference levels. Using the selection criteria yields some tendency towards negative values and negative jumps in the mean values for  $\Delta NEE$  60-100 m, whereas such an effect is not apparent for  $\Delta NEE$  100-180 m. Median values and selection criteria lead to similar results, where calculating the median either smoothens out or intensifies signal compared to applying the mean. Advective flux for the selection is about  $-0.2$ - $0.1 \text{ mg m}^{-2} \text{ s}^{-1}$ .

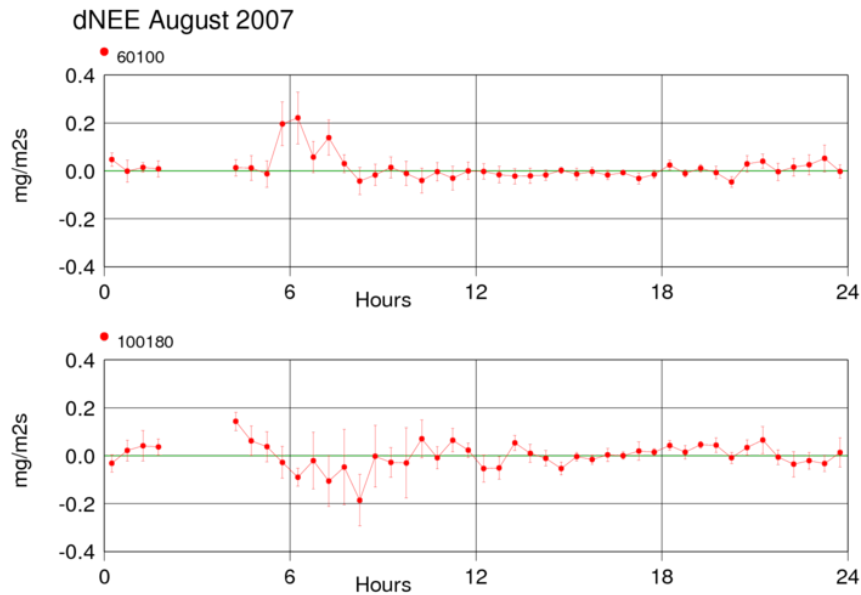


Figure 23. Average diurnal cycle (UTC) of  $\Delta NEE$  ( $\text{mg m}^{-2} \text{ s}^{-1}$ ) for August 2007. Upper panel shows  $\Delta NEE$  between 60 and 100 m. Lower panel shows  $\Delta NEE$  between 100 and 180 m. Error bars display standard error in the mean per 30-minute time interval.

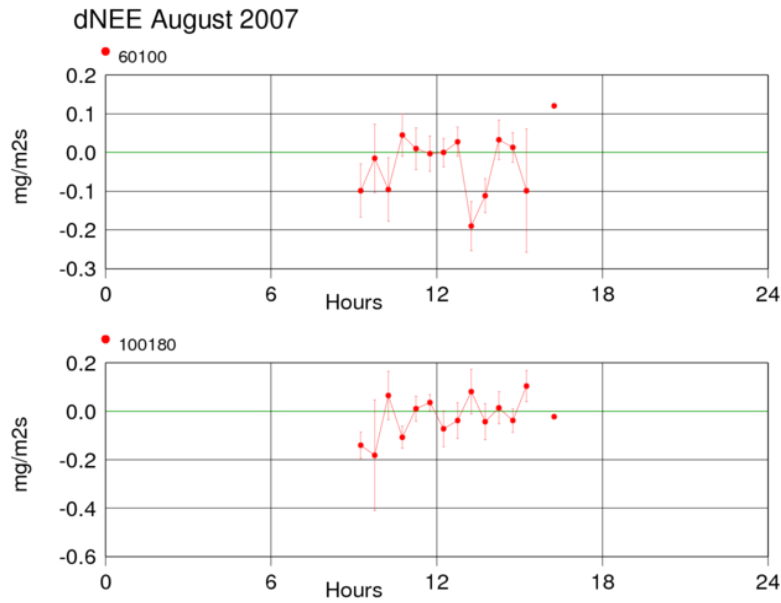


Figure 24. Average diurnal cycle (UTC) of  $\Delta NEE$  ( $\text{mg m}^{-2} \text{s}^{-1}$ ) for August 2007 with selection criteria for time (9-16 UTC),  $NEE$  60m ( $< -0.3 \text{ mg m}^{-2} \text{ s}^{-1}$ ) and ratio shortwave down radiation/clear sky radiation ( $> 0.7$ ). Upper panel shows  $\Delta NEE$  between 60 and 100 m. Lower panel shows  $\Delta NEE$  between 100 and 180m. Error bars display standard error in the mean per 30-minute time interval.

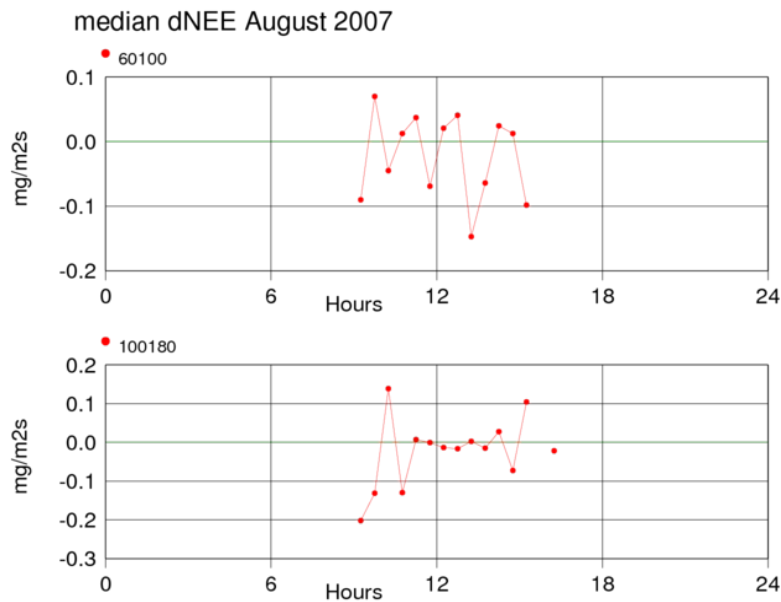


Figure 25. Diurnal cycle (UTC) of median values  $\Delta NEE$  ( $\text{mg m}^{-2} \text{ s}^{-1}$ ) for August 2007 with selection criteria for time (9-16 UTC),  $NEE$  60m ( $< -0.3 \text{ mg m}^{-2} \text{ s}^{-1}$ ) and ratio shortwave down radiation/clear sky radiation ( $> 0.7$ ). Upper panel shows  $\Delta NEE$  between 60 and 100 m. Lower panel shows  $\Delta NEE$  between 100 and 180m.

In summary, a typical range for the monthly averaged advective contribution is approximately 10% to 20% of NEE. During most monthly averaged diurnal cycles both CO<sub>2</sub> enriched and CO<sub>2</sub> depleted air is advected past the tower in a more or less alternating fashion. The signal is often significant for certain hours of a mean diurnal cycle, but also shows considerable noise in general. However, daytime data for May 2008 showed a significant and persistent trend indicating the advection of CO<sub>2</sub> enriched air at both height intervals. The daytime data under fair weather and under all-weather conditions are similar. At night depleting advection is most frequent and can sometimes be quite strong, around 40% of NEE, especially towards the early morning. Moreover, a striking advective phenomenon seems to often occur during the morning transition. It appears that a morning surge of depleting advection at the lower levels precedes a strongly enriching advective event at the higher levels. The magnitude of these advective fluxes can reach ~60% of NEE.

### 3.2.2. $\Delta$ NEE VERSUS WIND DIRECTION

$\Delta$ NEE data is related to wind direction in the section below, where results are obtained using the standard sampling criteria for NEE, sunlight and time.  $\Delta$ NEE 60-100m is compared to the wind measurement at 80 m height and  $\Delta$ NEE 100-180m to the 140 m wind measurement. During the months of April-June 2008 the easterly sector with wind directions of approximately 60-120° favors enriching advection, both between 60-100 m and between 100 and 180 m. Negative  $\Delta$ NEE occurs more frequently and values are greater in absolute magnitude. Wind directions of approximately 70-90° are significantly linked to negative flux at heights between 60 and 100 m. Yet, these results also suggest a connection between winds blowing from ~90-120° and positive advective flux. Data from the northwesterly sector (315 ± 30°) are filtered out because of reasons mentioned in the methods section. When the wind changes from a southerly direction (~180°) to westerly (~270°) an apparent general shift can be observed in the left panel of Figure 26. Between 60 and 100 m height the advective flux is predominantly positive and relatively high when winds blow roughly from 180-220°. Wind directions with a more westerly component appear to be related to enriching advection looking at the 60-100 m level. The distribution of data point seems to progressively incline towards negative values with an increasing westerly wind component. Unfortunately, there are no data for the northwesterly sector to further assess this feature. Figure 26 does not show such a distribution for the 100-180 m level. Advective flux data is more evenly divided between negative and positive sign and across wind directions between south and west. However, positive data points in this wind sector are more frequent. Directions of roughly 360-030° appear to be mostly associated with enriching advection. Since each data point represents only 30 minutes on a 3 month time scale, and because of limited data, most other wind directions do not give significant indications about advection in this assessment for April-June 2008.

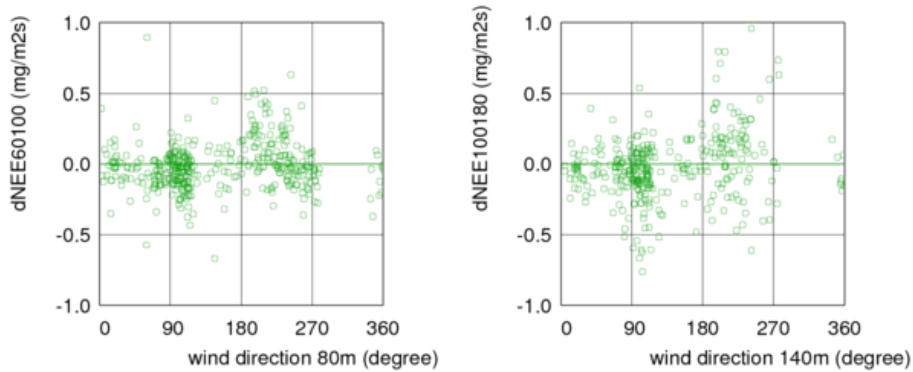


Figure 26. 30-minute measurements of wind direction ( $^{\circ}$ ) versus calculated  $\Delta NEE$  ( $\text{mg m}^{-2} \text{s}^{-1}$ ) with standard selection criteria during April 2008-June 2008. Left panel shows  $\Delta NEE$  between 60-100 m vs. wind direction at 80 m. Right panel shows  $\Delta NEE$  between 100-180 m vs. wind direction at 140 m.

In Figure 27, showing  $\Delta NEE$  versus wind direction during July-September 2007, some reoccurring features can be detected compared to April-June 2008. At the 60-100 m level with a wind direction of about 180-220 $^{\circ}$  the advective flux is significantly positive. Again, a westerly component in the south to west sector stimulates negative flux at this level. Such a pattern cannot be derived from the results for the 100-180 m level, where positive and negative values are quite balanced. The right panel in Figure 27 shows some tendency towards negative flux at 100-180 m when the wind direction is about 360-030 $^{\circ}$ , which was also attributed to the period of April-June 2008. Unfortunately, this data retrieval yielded very limited results for easterly winds making a comparison with other months impossible. Apart from southeasterly winds ( $\sim 120-150^{\circ}$ ) at 100-180 m which appear to result in negative fluxes, the remaining wind directions are either data limited or do not suggest predominantly enriching or depleting advective contribution.

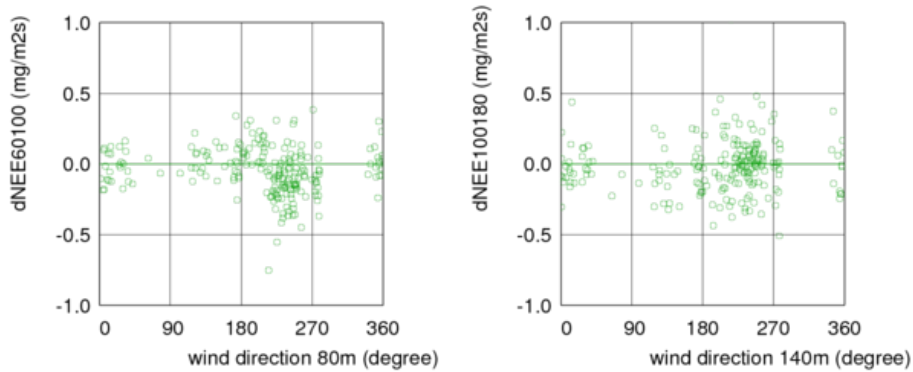


Figure 27. 30-minute measurements of wind direction ( $^{\circ}$ ) versus calculated  $\Delta NEE$  ( $\text{mg m}^{-2} \text{s}^{-1}$ ) with standard selection criteria during July 2007-September 2007. Left panel shows  $\Delta NEE$  between 60-100 m vs. wind direction at 80 m. Right panel shows  $\Delta NEE$  between 100-180 m vs. wind direction at 140 m.

Easterly winds prevailed during May 2008, which can also be seen in the scatter of Figure 28. With the exception of a few anomalous data points, enriching advection dominated at both levels under standard sampling conditions with wind directions ranging from north ( $360^{\circ}$ ) to east ( $90^{\circ}$ ). From  $90^{\circ}$  to about  $120^{\circ}$  these results also indicate positive flux, but negative values represent the vast majority and are of greater absolute magnitude. Figures 17-19 showing the average diurnal cycle of  $\Delta NEE$  also suggested an important role for enriching advection during this month. Note that upon reaching  $90^{\circ}$  an apparent sharp transition occurs, which is most pronounced at the 60-100 m level. Wind directions of  $> 90^{\circ}$  are also related to relatively high positive flux, whereas slightly backing winds are typically related to negative flux. This phenomenon is visible on a larger timescale as well in Figure 26 showing these data for April-June. Looking at other wind directions, only the southwesterly sector stands out where a significantly positive peak can be seen at approximately  $240^{\circ}$ .

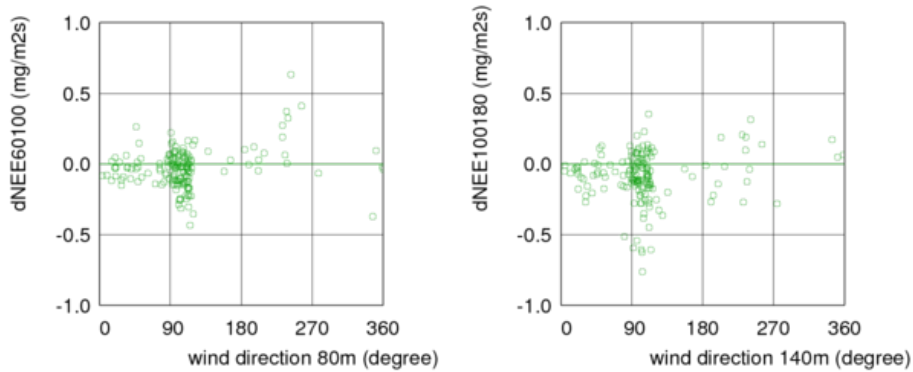


Figure 28. 30-minute measurements of wind direction ( $^{\circ}$ ) versus calculated  $\Delta NEE$  ( $mg\ m^{-2}\ s^{-1}$ ) with standard selection criteria during May 2008. Left panel shows  $\Delta NEE$  between 60-100 m vs. wind direction at 80 m. Right panel shows  $\Delta NEE$  between 100-180 m vs. wind direction at 140 m.

June 2008 (Fig. 29) is characterized by variable advective contribution, which was also shown in the average diurnal cycle results. In terms of wind direction the previously mentioned shift in flux sign between southerly and westerly direction can be seen at the 60-100 m level. In the southwesterly sector mostly negative flux values can be seen in figure at the 100-180 m level.

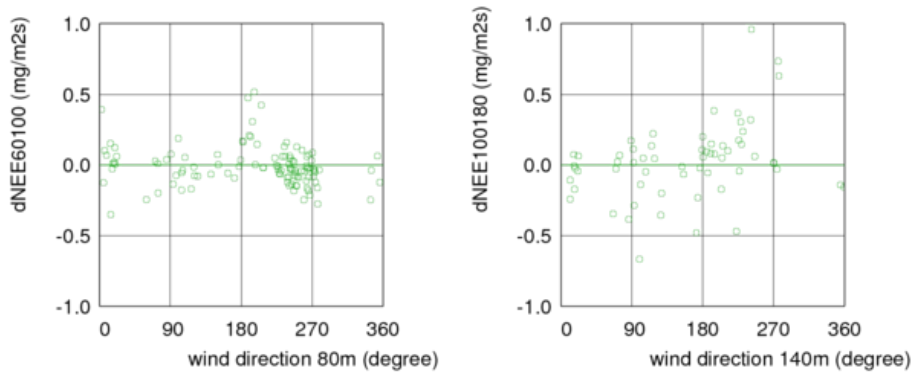


Figure 29. 30-minute measurements of wind direction ( $^{\circ}$ ) versus calculated  $\Delta NEE$  ( $mg\ m^{-2}\ s^{-1}$ ) with standard selection criteria during June 2008. Left panel shows  $\Delta NEE$  between 60-100 m vs. wind direction at 80 m. Right panel shows  $\Delta NEE$  between 100-180 m vs. wind direction at 140 m.

August 2007 had considerable variability in  $\Delta NEE$  at both levels as well. Figure 30 shows some similarity to the previous results looking at the south to west sector at the 60-100 m level though. Directions of approximately 170-220° are slightly dominated by positive flux between 60 and 100 m, whereas a wind direction roughly 230-280° shows more enriching advection at this level. This is most apparent between 270° and 280° at the 60-100 m level, where solely negative values are retrieved. As was already mentioned in the results for the 3-month assessment for July-September 2007 some tendency towards enriching advection with southeasterly (~120-150°) winds can be seen at 100-180 m in Figure 30.

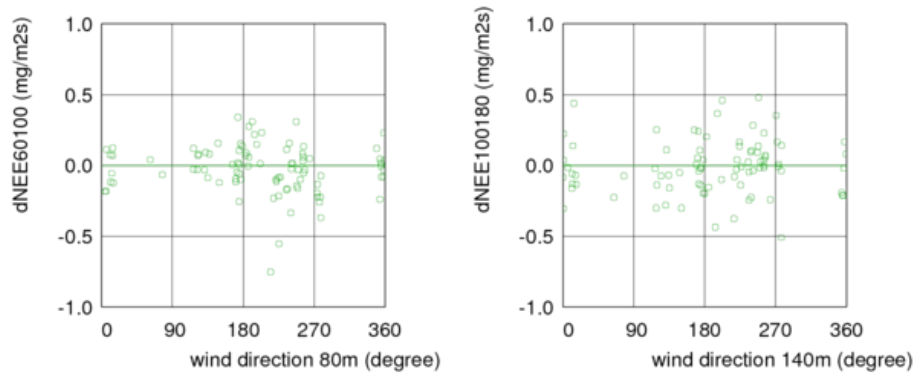


Figure 30. 30-minute measurements of wind direction (°) versus calculated  $\Delta NEE$  ( $\text{mg m}^{-2} \text{s}^{-1}$ ) with standard selection criteria during August 2007. Left panel shows  $\Delta NEE$  between 60-100 m vs. wind direction at 80 m. Right panel shows  $\Delta NEE$  between 100-180 m vs. wind direction at 140 m.

In summary, when only observing data under fair weather conditions, a given wind direction is not exclusively linked to either the advection of  $\text{CO}_2$  enriched or depleted air masses. It thus appears that, given a certain wind direction, the upwind source/sink-inhomogeneity of the Cabauw surroundings is such that with a range of conditions (e.g. atmospheric stability and unknown environmental factors) a combination of both enriching and depleting advective contribution can be expected at Cabauw. An exception to the latter may be occurring when winds blow from a direction of  $\sim 75^\circ$ . At the 60-100 m level the advection then appears to almost solely enrich the air masses. Also, when looking at larger ranges of wind directions (sectors), some interesting patterns can be observed. Winds from the easterly sector coincide most frequently with enriching advection (both levels). At the lower level a transition from predominantly depleting to predominantly enriching advection was found, going from the southerly to the westerly sector.

### 3.2.3. ATTRIBUTING ADVECTION TO STORAGE AND TURBULENT FLUX

Advective flux ( $\Delta NEE$ ) is explained by differences in storage flux ( $dFst$ ) and by the turbulent flux divergence ( $dFec$ ) when the latter two do not cancel each other out. An analysis of these contributions is provided here, where the data were retrieved using standard sampling criteria.  $dFst$  is simply the storage flux of the lower reference height minus that of the upper reference height and therefore represents the negative storage flux between levels (60-100 m and 100-180 m).  $dFec$  is the turbulent flux divergence taken as the eddy covariance measurement of the lower level minus that of the upper level, again for 60-100 m and 100-180 m. From Figures 31 and 32, showing data for the periods of April-June 2008 and July-September 2007 respectively, it becomes clear that the turbulent flux divergence is the major contributor to the  $\Delta NEE$  signal. An almost negligible portion of the  $dFst$  data fits the diagonal 1:1 line, whereas  $Fec$  versus  $\Delta NEE$  shows excellent correlation. In fact, enriching advection frequently coincides with a decrease in storage, which is likely related to the late morning hours and early afternoon. The opposite occurs less frequently. Only a minor part of the depleting advective flux data can, at least partly, be explained by the change in storage. Negative advective flux can to an even smaller extent be attributed to the storage flux.

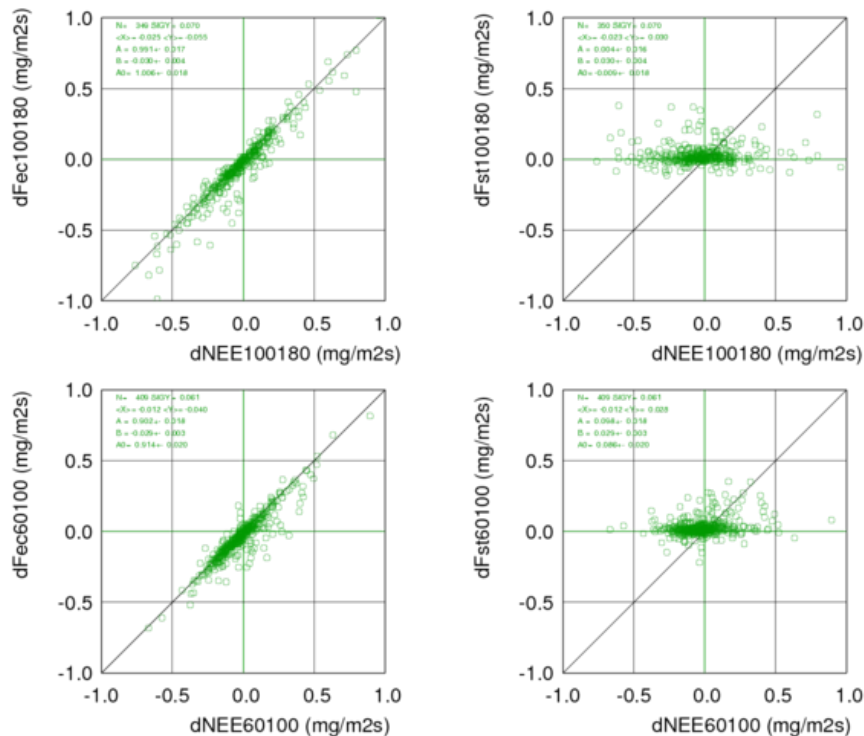


Figure 31. 30-minute measurements of turbulent flux divergence ( $dFec$ ) versus calculated  $\Delta NEE$  and 30-minute measurements of storage flux difference ( $dFst$ ) versus calculated  $\Delta NEE$  during April-June 2008. Upper panels give results for the 100-180 m level and lower panels for the 60-100 m level (all data in  $mg\ m^{-2}\ s^{-1}$ ). Standard selection criteria were applied in data sampling.

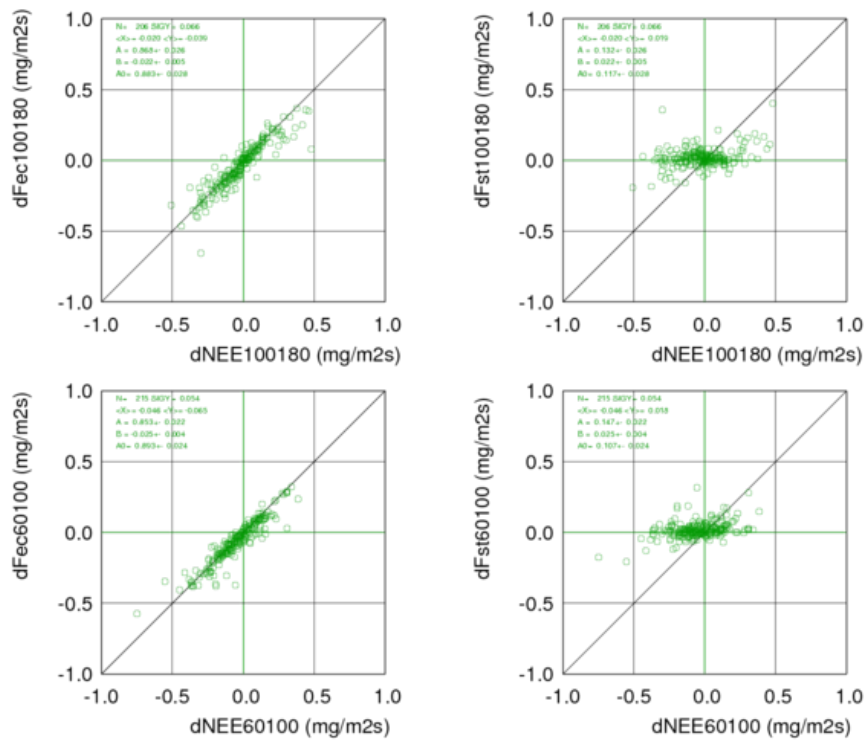


Figure 32. 30-minute measurements of turbulent flux divergence (dFec) versus calculated  $\Delta NEE$  and 30-minute measurements of storage flux difference (dFst) versus calculated  $\Delta NEE$  during July-September 2007. Upper panels give results for the 100-180 m level and lower panels for the 60-100 m level (all data in  $\text{mg m}^{-2} \text{s}^{-1}$ ). Standard selection criteria were applied in data sampling.

In summary, under fair weather conditions advection is reflected by differences in vertical turbulent fluxes along the Cabauw tower. Changes in storage play a minor role. This finding suggests that fair weather advection mainly originates from differences in turbulent flux footprints around the tower and not from concentration profiles being advected past the tower [Yi *et al.*, 2000]. If a minor part of the fair weather advection is reflected by changes in storage, this is mainly valid for the advection of  $\text{CO}_2$  depleted air masses, and it does not happen often.

### 3.2.4. CONCENTRATION VERSUS WIND DIRECTION

Advection can have a noticeable effect on the  $\text{CO}_2$  concentration, where depleting advection would cause relatively low concentrations and enriching advection would maintain relatively high concentrations, e.g. compared to the impact of net daytime uptake. However, determining a baseline excluding advection to

distinguish high from low concentration is challenging, because of high daily variability due to many unknown factors determining the NEE and the diurnal temporal concentration evolution. On a monthly timescale this variability leads to a non-straightforward approach in determining a typical diurnal baseline. Nonetheless, in this case the monthly averaged diurnal concentration cycle of May 2008 is compared to measurements of concentration versus wind direction. The latter data for May, sampled using all standard selection criteria, are given below in Figure 33. The monthly averaged concentration range from 0900-1600 UTC during May was about 388-395 ppm (not shown here). This is assumed to represent a normal concentration range, where advection effects are more or less balanced and thus serves here as a baseline. An important consideration in the assessment should be that, although the same part of the diurnal cycle is used, no selection criteria for NEE or sunlight were applied for the average diurnal cycle. Therefore, the concentration measurements given below are anticipated to generally be in the lower part of the baseline range or to be relatively low. Most apparent in Figure 33 is the difference in concentration range between the north-northeasterly and the east-southeasterly wind sector. Concentration data with wind directions of  $0^{\circ}$  to approximately  $70^{\circ}$  are spread apart by just a few ppm and clustered in the lower part of the 388-395 ppm range. In contrast to this, concentration measurements with a wind direction roughly  $70$ - $120^{\circ}$  are spread well above and below the 388-395 ppm range. Previous observations of  $\Delta$ NEE versus wind direction could be related to this. The east to southeasterly sector showed a dominant role for relatively strong enriching advection, but also indicated times where advection was persistently depleting. Such a combination might be linked to a large concentration range as shown in these data. Less persistent advective flux of lower magnitude and of non-constant sign may be associated with more tightly clustered concentration measurements, such as observed for the north-northeasterly sector. Because other wind directions show very few data for May, these are not discussed.

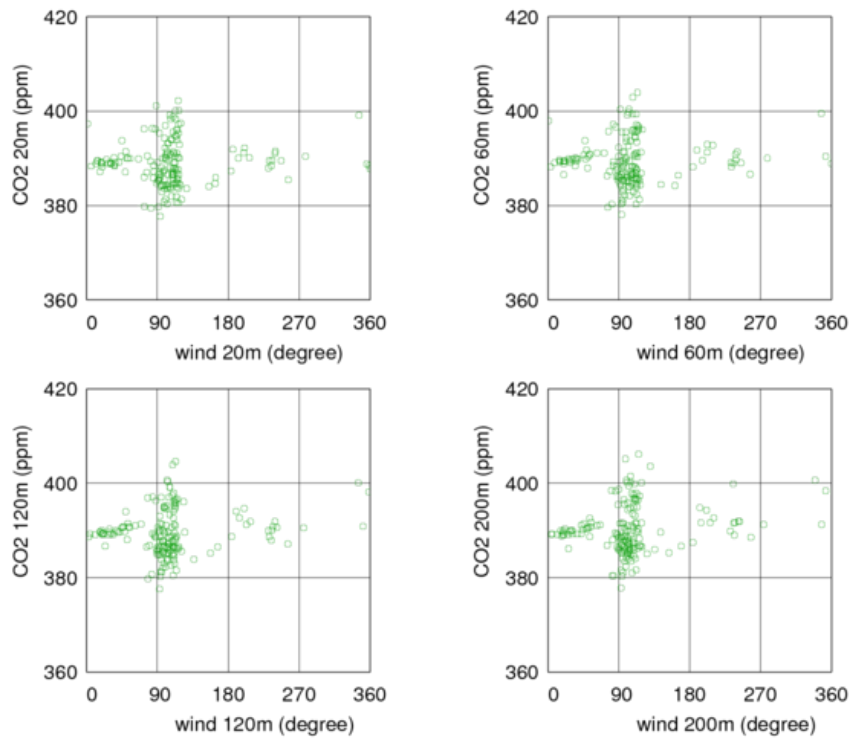


Figure 33. All 30-minute interval measurements of wind direction ( $^{\circ}$ ) versus concentration (ppm) at 4 measurement levels (20, 60, 120 and 200 m) during May 2008; sampled with standard selection criteria for time (9-16 UTC), NEE ( $< -0.3 \text{ mg m}^{-2} \text{ s}^{-1}$ ) and ratio shortwave down radiation / clear sky radiation ( $> 0.7$ ).

The results for  $\Delta$ NEE 60-100 m versus wind direction suggested a general tendency shift from depleting advection to enriching advection, going from southerly to westerly winds. This apparent effect might be reflected in results showing concentration versus wind direction. Unfortunately, all months of the summer half year under study contained very limited data in this wind sector, likely due to the selection criteria, not allowing a fair comparison. In addition, sometimes the opposite of the expected differences in concentration were observed for this wind sector. To exemplify this, data for June 2008 are given below in Figure 34. Based on the advection observations, a transition may be anticipated with relatively low concentrations between southerly and southwesterly direction, and relatively high concentrations from southwesterly to westerly winds. June nor the other monthly concentration results support these findings. Figure 34 shows a similar concentration range in these wind sectors, where the mean concentration around  $\sim 200^{\circ}$  is even higher than around  $\sim 240^{\circ}$ . Two relatively dense data clusters, positioned at roughly  $240^{\circ}$  and  $270^{\circ}$ , do mutually comply with the observed  $\Delta$ NEE trend. However, taking into account the large

data deficiency this observation should be considered weak. With the exception of May, the months studied also yielded very limited data for the other wind sector of particular focus: easterly winds. Therefore, these are not further addressed. The results do support the previously stated assumption that these concentration measurements would generally be in the lower range of the concentration range derived from the monthly averaged diurnal cycle (0900-1600 UTC). The latter range was 384-392 ppm for June (not shown here).

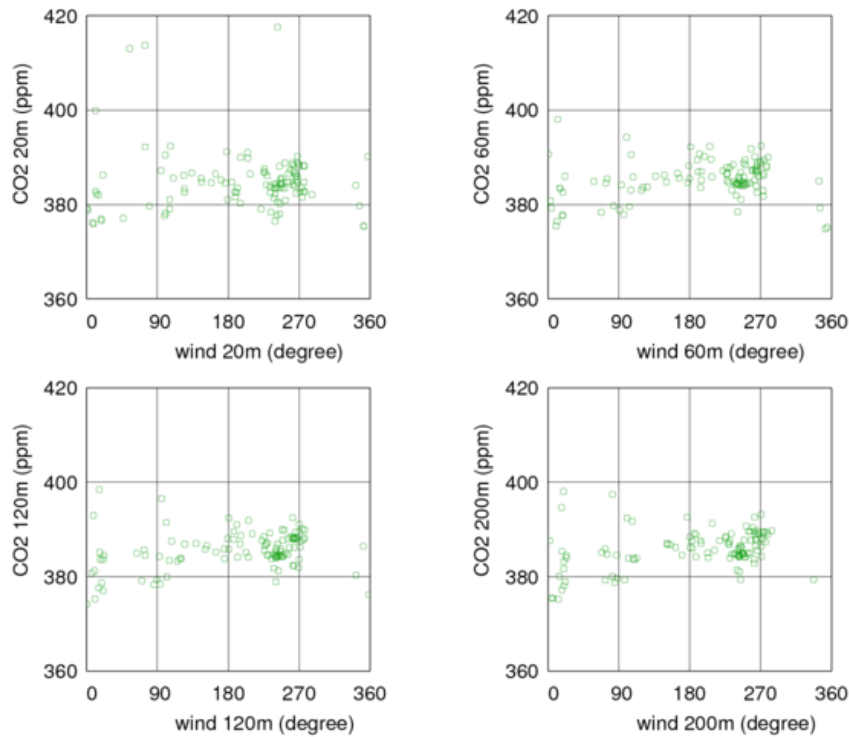


Figure 34. All 30-minute interval measurements of wind direction ( $^{\circ}$ ) versus concentration (ppm) at 4 measurement levels (20, 60, 120 and 200 m) during June 2008; sampled with standard selection criteria for time (9-16 UTC),  $NEE (< -0.3 \text{ mg m}^{-2} \text{ s}^{-1})$  and ratio shortwave down radiation / clear sky radiation ( $> 0.7$ ).

### 3.2.5. SOURCE AND SINK AREAS

We have assessed the potential  $\text{CO}_2$  sources and sinks in the Cabauw surroundings based on a satellite image of land cover (source: *Aerodata*, 2011). This image, dating from April 2007, is given below in Figure

35. Note: the footprint distance estimations mentioned in this section are explained in section 2.5 and given in Table I. The wind direction areas of interest will be addressed clockwise, starting north. The main focus will be on 4 wind sectors (Figure 35; color shaded areas) which showed interesting advective features, mentioned in section 3.2.2. In between the north and the red shaded area, starting at roughly 70°, no substantial evidence for either a dominant role for enriching or depleting advection was found. Figure 35 shows that in the immediate surroundings of the mast in this sector, in the order of hundreds of meters, grassland dominates. At distances exceeding about 500-700 m the edges of the village of Lopik emerge, which can act as a relative source of CO<sub>2</sub> for the tower. Behind this urban area, at distances ~ > 1 km, grassland again dominates and is mixed with some patches of arable land. On the total footprint scale of about 2300 m (see: Table I and section 2.5) this sector might be seen as moderately heterogeneous, and lead to a mix of enriching and depleting advection with no extremes.

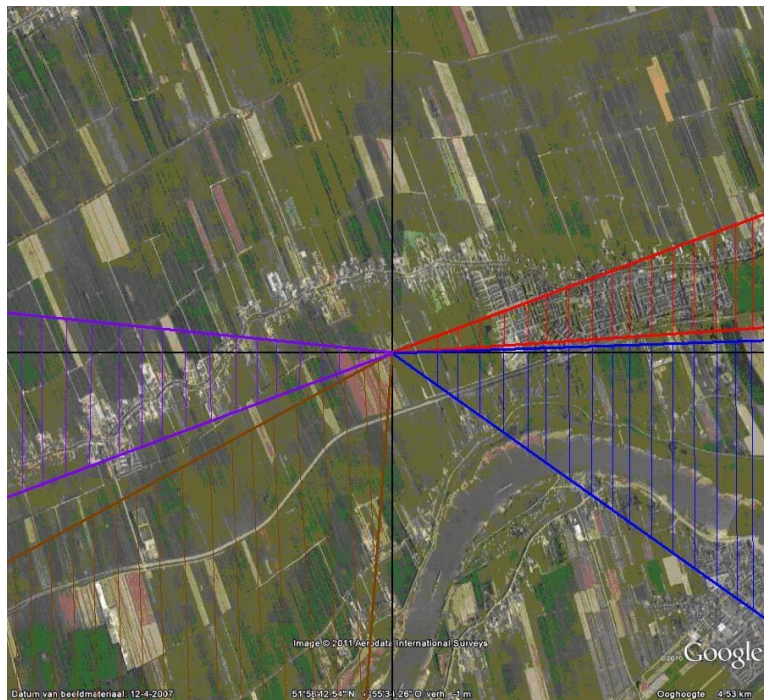


Figure 35. Satellite image obtained from Google Earth showing the Cabauw surroundings. Photograph was taken on April 12<sup>th</sup> 2007. The measurement site is located at the center of the black cross-hairs, which indicate north, east, south and west. Image is orientated to the north. Lateral distance from the center to the edge of the picture is about 2.5 km. Aerodata, 2011.

Arriving in the wind sector marked in red, roughly 70-85°, the fetch over urban Lopik strongly increases. In this direction the village starts at about 500-700 m from the mast and continues for another 1,5 km. This implies that the influence of Lopik, acting as a CO<sub>2</sub> source, becomes greater when winds blow from

these directions. The peak location of the 100 m level footprint lies in the center of the urban area. This could explain the  $\Delta NEE$  observations in this wind sector, where advection was found to be significantly enriching between 60 and 100 m height. A similar effect for the 100-180 m level is less clear, looking in this direction. In the blue shaded area in Figure 35, roughly bounded between  $85^\circ$  and  $120^\circ$ , a wide variety of land cover can be seen, as apposed to the previous situation with a long fetch over Lopik. The blue area comprises the pastures directly surrounding the tower, the urban borders of Lopik, agricultural land, the Oerlemans forest, the river Lek with its floodplains and the town of Ameide. Perhaps therefore, this area could be regarded as relatively heterogeneous compared to an all-grassland situation. This is then supported by the  $\Delta NEE$  data showing both significant enriching and depleting advection. It is also consistent with the observed transition from a dominance for enriching to a mix of both enriching and depleting advection between 60 and 100 m at about  $85^\circ$ . Unfortunately, considering the degree of variability in the  $\Delta NEE$  data it is hard to pinpoint specific land features using the footprint estimations. Data in between the blue area and the area shaded in brown was very limited and are therefore not discussed. Wind directions between south and west though showed an interesting feature, because of a shift from predominantly depleting to enriching advection at the 60-100 m level. Within the total wind direction range of south to west 2 sectors are designated in Figure 35, being brown ( $\sim 185-240^\circ$ ) and purple ( $\sim 245-275^\circ$ ). After a general inspection the brown sector appears to be relatively homogeneous compared to e.g. the blue one, since it is mostly comprised of grassy meadows and some arable land patches. The purple area is different, because of the urban influence of the village of Cabauw. Bearing in mind that the footprint peak location of the 60 m level should be about 750 m from the mast and 1250 m for the 100 m reference height, a suggestion can be made to explain the  $\Delta NEE$  observations. Doing so, the main clue for the brown area comes from the fallow land (brownish, rectangular shaped) directly lying to the southwest of the measurement site. This patch, assumed to take up less  $CO_2$  than the grassland farther away, could influence the 60 m measurement such that depleting advection is measured. It influences the tower only when winds blow roughly from the south to approximately west, with a maximum fetch over this patch at about  $200-210^\circ$ . The maximum fetch more or less corresponds with the maximum  $\Delta NEE$  values observed in section 3.2.2. As the westerly wind component increases, the relative contribution from this fallow land might diminishes, because more grassland is incorporated in the lower level footprint. Approaching the purple wind sector a combination of enriching and depleting advection was observed with no clear boundary. It is possible that the decreasing fetch over the fallow land, combined with an increasing role of the urban area of Cabauw, causes the transition from depleting to enriching advection, going south to west. In that case the 60 m measurement level progressively incorporates more grassland into its footprint, whereas the 100 m level is anticipated to be influenced more by the village of Cabauw in the purple sector. The northwesterly wind sector cannot be discussed, because it was filtered out for reasons mentioned in the methods section.  $\Delta NEE$  data in between northwesterly and northerly direction was limited and did not suggest any significance. It is therefore not discussed.

## **4. DISCUSSION AND CONCLUSIONS**

From CO<sub>2</sub> flux and concentration observations at a number of levels in the lowest 200 m of the atmosphere we have tried to estimate CO<sub>2</sub> advection. This was done at the 213 m high tall-tower near Cabauw, The Netherlands. CO<sub>2</sub> advection is often assumed to be negligible under convective conditions over relatively homogeneous and flat terrain. This measurements site, with its fairly ideal surroundings, serves as a suitable test-bed to assess the validity of this assumption for Cabauw and similar landscapes. In addition to advection estimations, this study focused on describing temporal and vertical variability of CO<sub>2</sub> concentration and fluxes at this site. Monthly averaged diurnal data from July 2007-June 2008 were analysed.

### **4.1. CO<sub>2</sub> CONCENTRATION**

The CO<sub>2</sub> concentration close the land surface was found to be typically variable within a monthly averaged diurnal cycle. At night, with a stable atmospheric boundary layer and low-wind conditions, CO<sub>2</sub> accumulates near the surface due to respiration. This leads to relatively high nocturnal concentrations and a significant vertical concentration gradient. During the day concentrations are relatively low because of photosynthetic CO<sub>2</sub> uptake. Convective mixing leads to a near-uniform vertical concentration profile during daytime. The duration of such a profile in monthly averaged diurnal cycles was found to be proportional to the mean monthly daylight time. However, observations for December deviated from this trend. Mean diurnal concentrations during December were relatively constant and a negative vertical concentration gradient was maintained. At a height of 20 m the minimum mean daytime concentration during December was ~408 ppm, which constitutes the maximum daytime concentration of the year studied. The minimum mean daytime concentration of ~376 ppm was observed during August. Mean diurnal concentrations during months in between December and August were intermediate. The nocturnal maximum mean concentration at 20 m height did not show an obvious seasonal pattern and was relatively constant between seasons. It ranged from 403 to 420 ppm between months. Consequently, the largest night versus day concentration difference at 20 m height was observed during August (~40 ppm). This difference was about 10 ppm during December. Concentrations at higher levels were observed to be more closely coupled to the daytime concentration minimums, which is due to weak mixing at night. Overall, wintertime is dominated by CO<sub>2</sub> respiration and summertime by CO<sub>2</sub> assimilation [Davis *et al.*, 2003], which corresponds with the observed seasonal differences. By the end of summer a maximum in terrestrial biomass and soil temperature is typically reached [Davis *et al.*, 2003]. It is believed that the August

daytime concentration minimum is related to the biomass maximum, due to high accumulated assimilation over the northern hemisphere. High nocturnal soil temperature and a large biomass (high respiration rates) may explain the large differences between daytime and night-time concentration at 20 m during summer. During December, daytime stable atmospheric stratification and minor assimilation, due to the December sunlight minimum and low biomass, are believed to be linked to the daytime maximum at 20 m height. Additionally, during December the yearly soil temperature minimum is yet to be reached later in winter. This may contribute to the 20 m concentration peak, because of relatively high respiration compared to other winter months. But these analyses are outside the scope of this study.

## 4.2. CO<sub>2</sub> FLUXES

At night the vertical turbulent flux at 5 m height ranged typically between +0.2 and +0.3 mg m<sup>-2</sup> s<sup>-1</sup> during the spring and summer months of e.g. May, July and August. This indicates respiration and upwards transport of CO<sub>2</sub> from the ground. At higher levels the nocturnal vertical turbulent flux during these months was usually lower in magnitude than at 5 m, because of weak mixing. The subsequent vertical turbulent flux divergence mainly causes the accumulation of CO<sub>2</sub> near the surface and the concentration gradient at night mentioned previously. This was fairly accurately reflected by the storage fluxes. During December nights the 5 m flux was approximately +0.1 mg m<sup>-2</sup> s<sup>-1</sup> and was not significantly different from higher levels. Less divergence during December in part explains the relatively constant concentrations observed. During morning hours a transition typically occurs when a stable nocturnal boundary layer evolves to a convective and well-mixed boundary layer exceeding the tower height. This period involves negative turbulent flux at 5 m due to assimilation at ground level, and positive fluxes (max. ~0.2 mg m<sup>-2</sup> s<sup>-1</sup> during summer) progressively reaching higher levels over time. Positive fluxes occur because CO<sub>2</sub> accumulated at night is mixed with relatively low CO<sub>2</sub> content air higher up. This morning transition vertical divergence leads to significant storage fluxes reaching magnitudes of -0.5 mg m<sup>-2</sup> s<sup>-1</sup> at the most during summer. After the morning transition vertical turbulent fluxes become negative at all levels under well-mixed conditions with net CO<sub>2</sub> uptake at the surface. The maximum mean 5 m height vertical turbulent flux is in the range of -0.04 to -0.07 mg m<sup>-2</sup> s<sup>-1</sup> during the summer half year. The storage fluxes are near-zero during daytime. Entrainment of relatively CO<sub>2</sub> rich air from the residual layer or free troposphere is believed to contribute to the negative turbulent fluxes at higher levels during the day [Casso-Torralba *et al.*, 2008]. The general diurnal flux pattern described above holds for most months studied. However, data for e.g. December did not show the daytime pattern, likely because of weak vertical mixing due to absence of predominant convective conditions.

### 4.3. CO<sub>2</sub> NET ECOSYSTEM EXCHANGE

Over 3-month periods during April-September - under fair weather daytime conditions - the mean net ecosystem exchange (NEE) estimated from 3 observational levels does not significantly deviate. Mean values are fairly constant at -0.4 to -0.5 mg m<sup>-2</sup> s<sup>-1</sup>. These values are reasonably consistent with the observed 5 m vertical turbulent fluxes. During monthly averaged diurnal cycles of the same summer half year, and covering all-weather conditions, the mean maximum daytime NEE values from the 3 observational levels were about -0.4 to -0.7 mg m<sup>-2</sup> s<sup>-1</sup>. These were also quite similar to the 5 m turbulent flux maximums. However, it was observed that averaged over 3-month periods - during fair weather daytime conditions - a slightly more negative NEE value occurs at subsequent lower levels, i.e. 60 m versus 100 and 100 versus 180 m. This could be caused by structurally enriching advection, or be related to turbulence statistics going higher up in the atmosphere [Stull, 2000a]. During monthly averaged diurnal cycles the NEE estimations are believed to be generally influenced by advection and inconsistency in flux measurements. Especially during the morning transition the NEE estimations deviated from the 5 m turbulent flux. This could be due to significant advective flux or an erroneous imbalance between vertical turbulent and storage flux measurements in this non-stationary phase. If the latter applies, the turbulent flux measurement error is believed to be the main cause. When the atmospheric layer along the tower is not well-mixed, e.g. during nights or wintertime, inaccurate storage fluxes may result from insufficient concentration measurement heights. This could consequently lead to faulty NEE estimations. Night-time and winter estimations of NEE during this study are believed to be accompanied by a degree of uncertainty due to these reasons. In addition to this, the NEE-model output versus observational NEE estimation inter-comparison showed significant deviation during virtually all phases of the monthly averaged diurnal cycles studied. This is especially valid for the morning transition. Around noon a minor anomaly between the model and the observational data was observed. It is not known whether the model or observational data are more reliable.

### 4.4. CO<sub>2</sub> ADVECTION

A non-negligible role for advection of CO<sub>2</sub> at the Cabauw site was found. This finding holds under fair weather conditions during daytime. Fair weather data were used to test the hypothesis of constant NEE with height for the relatively ideal situation at Cabauw. The same finding also holds for full diurnal cycles and all weather conditions. With an 'enriching flux' in the text below is meant that CO<sub>2</sub> rich air masses are advected past the tower (flux has negative sign). A 'depleting flux' means that CO<sub>2</sub> poor air masses are advected past the tower (flux has positive sign).

Averaged over 1-month or 3-month periods the advective contribution during daytime is mostly in the order of  $0.05\text{-}0.1 \text{ mg m}^{-2} \text{ s}^{-1}$ . This is about 10-20% of the average maximum value for the daytime NEE. However, the advective flux is not always persistent and statistically significant during monthly averages. It frequently exhibits important fluctuations around zero, but was also observed to be significantly and consistently of one sign during a few hours of a mean diurnal cycle. No significant differences were observed in this contribution between fair weather and all-weather conditions. The fair weather selection does cause a more erratic signal in the  $\Delta\text{NEE}$  data, which is likely due to data limitation. At times, the advective contribution to NEE may reach about 40%. However, this is not a frequent occurrence in these averaged results. It does support a previous finding by *Werner et al.* [2004], who suggested an upper-bound in the range of 30-60%. We find a typical advective contribution of approximately 20%, which is consistent with a daytime period studied by *Casso-Torralba et al.* [2008]. Monthly averaged daytime advection is usually alternately enriching and depleting and noisy, as in the case of June 2008 and August 2007. However, daytime advection can be predominantly and significantly of one sign (i.e. enriching or depleting) during the course of a month. May 2008 nicely demonstrates this, showing a persistent enriching flux at both the 60-100 m and 100-180 level. On a 3-month basis a similar, yet diminished, effect was observed for July-September 2007 in between 60 and 100 m height.

At night, the magnitude of mean advection is usually around  $0.05\text{-}0.1 \text{ mg m}^{-2} \text{ s}^{-1}$ , which constitutes about 20-40% of the nocturnal NEE. This advective flux is depleting on average, suggesting that relatively  $\text{CO}_2$  poor air may typically be advected past the tower at night. Additionally, late at night or very early in the morning some remarkable peaks of mean depleting advection events were observed. However, a degree of variability should be considered here, especially when looking at smaller time scales. During some monthly averaged diurnal cycles enriching advection also plays a significant role during individual days, and the signal can be quite noisy around the actual monthly means. For some months the significance of the  $\text{CO}_2$  depleting advective surges are therefore questionable.

The morning transition period was observed to coincide with strong advective phenomena. In many cases, advection is depleting between 60 and 100 m height, preceding a surge of enriching advection at the 100-180 m level. This is a pattern similar to findings by *Yi et al.* [2000] and *Werner et al.* [2004], who observed this at a site in the USA and at the Cabauw site, respectively. Maximum mean  $\Delta\text{NEE}$  values are approximately  $0.3 \text{ mg m}^{-2} \text{ s}^{-1}$ , or around 60% of the NEE in this investigation. *Werner et al.* [2004] found about 80% at the most.

These results provide an estimation of the total advective contribution, which in principle is composed of different components. It simply represents the residual term of the scalar conservation method used. For instance, separating horizontal from vertical advection is not done in this investigation. Other budget

terms being neglected in the methodology may still be of influence to the measured signal. One of these terms is the gradient of the horizontal turbulent flux. Because of the relatively homogeneous surroundings of Cabauw the horizontal flux divergence was assumed to be small, assuming the horizontal length scale is much larger than the depth of the atmospheric boundary layer. This horizontal length scale is defined by the heterogeneity of the landscape. Persistent spatial gradients in the horizontal turbulent flux can occur over heterogeneous land surfaces [Yi *et al.*, 2000]. It is possible that a degree of inhomogeneity of the Cabauw region contributes to the  $\Delta$ NEE estimations in terms of horizontal turbulent flux.

The actual total advective flux can ultimately come from: 1) heterogeneity in sources and sinks relevant to the footprint of the flux sensors; 2) concentration profiles being advected past the tower, and 3) perhaps large scale CO<sub>2</sub> transport by subsidence and convergence [Yi *et al.*, 2000]. Under the fair weather selection used in this study, a well-mixed atmospheric layer exceeding the mast height should stimulate accurate measurements. This is because of the associated quasi-stationary situation, where turbulent flux and concentration measurements are relatively stable over time [Stull, 2000a; Casso-Torralba *et al.*, 2008]. The results of this study with fair weather selection indicate that differences in turbulent flux with height, and not the differences in storage flux, cause the  $\Delta$ NEE. Therefore, the causes of advection may be sought in differing turbulent flux footprints around the tower. Two wind sectors were identified in which the observations tend to show this behaviour: an easterly sector and a south-westerly sector. In general, the easterly sector has an enriching effect at both height intervals, where the town of Lopik is assumed to be the main contributor. The reason for advection from the south-westerly sector is less clear, but a nearby agricultural field and the town of Cabauw may be related to this observation. When winds change from southerly to westerly direction a transition from depleting to enriching advection at the 60-100 m level was observed. This transition could be potentially explained if the agricultural field is fallow land during springtime and covered with maize during summertime. However, this study did not analyse land-use in temporal detail and so, this would need to be further assessed. The enriching effect with easterly winds is reflected by persistent advective flux during May 2008, when winds blew predominantly from the east. Variability in the sign and magnitude of  $\Delta$ NEE with constant wind directions is likely related to differing sizes and locations of flux footprints. In this investigation footprint peak location estimates were used based on neutral atmospheric stability conditions. Therefore, with changing stability conditions the footprint peak relocates causing uncertainty in the distances used in this study. A similar effect comes from the size and shape of the footprints (not assessed in this study). If the spatial scale of the heterogeneous surface patches is similar to the spatial scale of the footprint, the advective effect will be relatively large. If the footprint is large compared to the heterogeneous surface patches, the advective effect will be washed out more by large scale eddies [Yi *et al.*, 2000]. The relative contribution of vertical turbulent flux and storage flux under all-weather conditions was not analysed, and is therefore not discussed. Extreme  $\Delta$ NEE during the morning transition may be related to horizontal advection after night

time pooling in the nearby region, following a suggestion by *Yi et al.* [2000], or vertical advection. However, the non-stationary situation associated with the morning transition potentially leads to faulty measurements.

Because of the statistical nature of vertical turbulent flux measurements some degree of error is inherent to this method. Higher up in the atmosphere, the eddies contributing to the measured turbulent flux become larger and pass by less frequently. This effect diminishes the statistical strength of eddy covariance measurements obtained high above the ground [*Stull, 2000a*]. Moreover, the flux sensors at Cabauw may structurally deviate by 3% over the course of months due to uncertainties in their calibrations. This error alone could account for an uncertainty in  $\Delta NEE$  of 5% of the turbulent flux. Since  $\Delta NEE$  is typically 20% of  $NEE$  this amounts to an uncertainty in  $\Delta NEE$  of 25%. Inaccurate storage fluxes can also result in over or underestimation of  $\Delta NEE$ . A cause for this may be that the limited amount of concentration measurement heights incompletely reflects the actual storage when vertical mixing is weak. This mainly applies for the  $\Delta NEE$  data without fair weather selection and especially during stable night-time conditions.

The estimations of advective contribution presented here should be an important consideration in  $NEE$  assessments for Cabauw and similar landscapes. It is shown that simply neglecting advection and applying [ $NEE = NEE_o$ ] can lead to erroneous  $NEE$  integrations over time, also for a relatively homogeneous landscape setting like at Cabauw.

## **ACKNOWLEDGEMENTS**

This work started out as a 4-month internship at KNMI as part of my Master's programme Climate Studies at Wageningen University. Along the way it was decided to extend the analyses and let it grow into my MSc thesis. The final 'condensed' result is this KNMI-technical report, which I presume you have just carefully read. A number of people played an important role on the road towards this manuscript, both on the technical and the more personal level. For these people, a word of thanks.

Alex Vermeulen (*ECN*, Petten) provided quality checked concentration data, which was an essential step in this research. Another significant data related contribution was made by Eddy Moors (*Alterra*, Wageningen) who provided the 100 m height turbulent flux measurements.

I especially thank my KNMI supervisor Fred Bosveld for his help on many points during this research, and for allowing me to do my MSc thesis at KNMI. I owe him gratitude for bringing me up to speed on some theoretical background, data access, using his software in the analysis, daily supervision and thorough scrutiny of this report. His patience during the writing phase, and understanding when progress was hampered due to personal circumstances, is also very appreciated. I also thank my university supervisor Laurens Ganzeveld for his critical look at my report, general supervision and stopping by at KNMI to discuss this project.

I am grateful to my parents Wil van Brederode and Ward Gerritsen who showed near-infinite patience during a rather lengthy period of study. As far as this thesis work is concerned their contribution from the sidelines was extremely important. Without their money injections at financially rough moments, making it to the finish of this thesis might have proven to be an impossible challenge. Many thanks for that and for the moral support and interest. I also thank my brother Roderik Gerritsen for his optimism, funny comments and empathy, which was also often exhibited online while we both worked behind a computer.

I anticipated that skipping our annual friend's Christmas dinner to write on this report would evoke lots of phone calls, text messages and e-mails showing several levels of outrage and alcohol intoxication. But instead, my friends paid me a visit bringing a wish-well card and dinner left-overs. Thanks again, Joost, Rens, Arjan, Ben, Niels, Susanne and Kim. My friend Roel Stappers played a role, both at and outside of KNMI. Too bad for me that you got a job abroad and left KNMI, making my cigarette breaks quite lonely. Thanks for all of our nice talks about the ups and downs of doing research, science and life in general. Finally, I want to mention my good and oldest friend Joris Haagen. Thank you for being a faithful ally at all times and for your steadfast and uplifting praise for the work that went into this thesis.



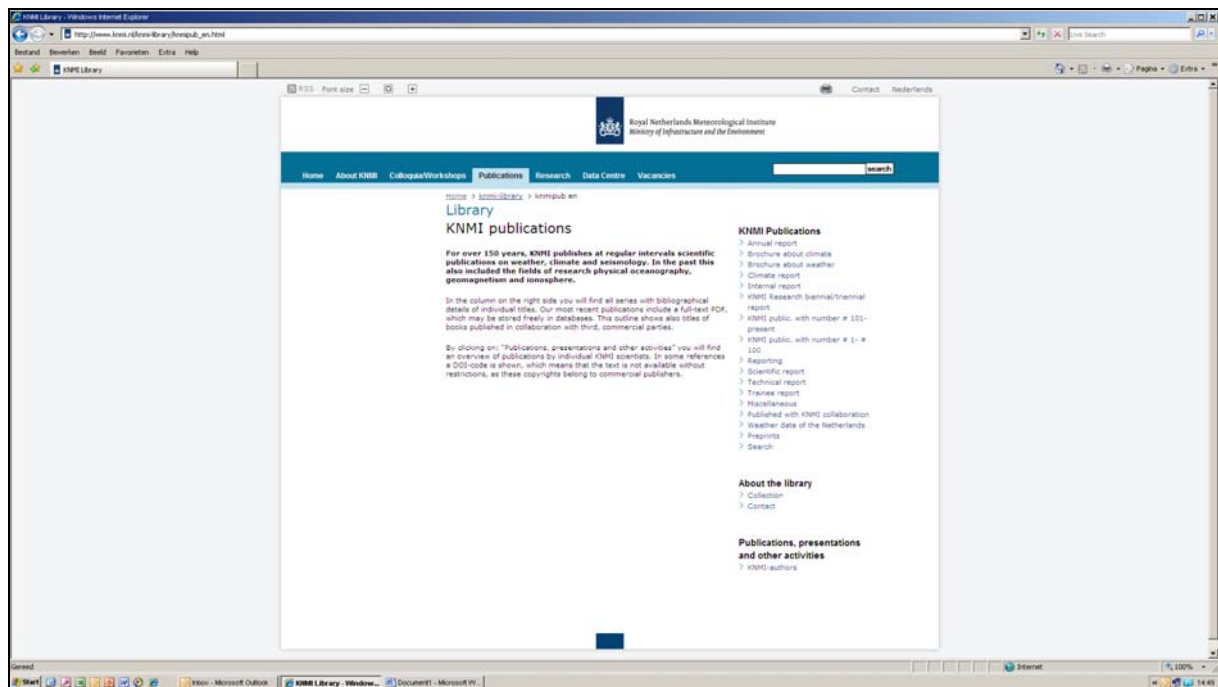
## REFERENCES

- Baldocchi *et al.* [2001]; FLUXNET: A new tool to study the temporal and spatial variability of ecosystem-scale carbon dioxide, water vapor, and energy flux densities; *Bulletin of the American Meteorological Society*, volume 82, No. 11, 2415-2435.
- Baldocchi *et al.* [2003]; Assessing the eddy covariance technique for evaluating carbon dioxide exchange rates of ecosystems: past, present and future; *Global Change Biology*, 9(4), 479-492.
- Beljaars and Bosveld [1996]; Cabauw data for the validation of land surface parameterization schemes; *Journal of Climate*, 10, 1172- 1193.
- Bosveld [2010] – online documentation; Cabauw observations, calibrations and MOBIBASE database software; <http://www.knmi.nl/~bosveld/>
- Casso-Torralba *et al.* [2008]; Diurnal and vertical variability of the sensible heat and carbon dioxide budgets in the atmospheric surface layer; *Journal of Geophysical Research*, Volume 113, D12119.
- Davis [1992]; Surface fluxes of trace gases derived from convective-layer profiles; Ph.D. dissertation; *NCAR cooperative thesis 139*, University of Colorado, Boulder.
- Davis *et al.* [2003]; The annual cycles of CO<sub>2</sub> and H<sub>2</sub>O exchange over a northern mixed forest as observed from a very tall tower; *Global Change Biology*, 9, 1278-1293.
- Friedlingstein *et al.* [2003]; How positive is the feedback between climate change and the carbon cycle?; *Tellus*, 55B, 2, 692-700.
- ICOS [2011] – online documentation; Integrated carbon observation system; <http://www.icos-infrastructure.eu/>
- IPCC [2007] – online documentation; Intergovernmental panel on climate change; 4<sup>th</sup> assessment report; <http://www.ipcc.ch/>

- Jacobs *et al.* [2007]; Variability of annual CO<sub>2</sub> exchange from Dutch grasslands; *Biogeosciences*, 4, 803–816.
- Kljun *et al.* [2004]; A simple parameterisation for flux footprint predictions; *Boundary-Layer Meteorology*, 112, 503-523.
- Schmid [2002]; Footprint modeling for vegetation atmosphere exchange studies: a review and perspective; *Agricultural and Forest Meteorology*, 113, 159–183.
- Stull [2000a; 1988]; An introduction to boundary layer meteorology; *Springer*, New York, USA.
- Stull [2000b]; Meteorology for scientists and engineers; second edition; *Brooks/Cole*, Pacific Grove, USA.
- Van Ulden and Wieringa [1995]; Atmospheric boundary layer research at Cabauw, *Boundary Layer Meteorology*, 78(1– 2), 39– 69.
- Webb *et al.* [1980]; Correction of flux measurements for density effects due to heat and water vapour transfer; *Quarterly Journal of the Royal Meteorological Society*; 106, 85–100.
- Werner *et al.* [2004]; The role of advection on CO<sub>2</sub> flux measurements at the Cabauw tall tower, the Netherlands; in *17th Symposium on Boundary Layers and Turbulence*, 2006, JP5.3, pp. 1– 8, San Diego, California, USA.
- Wilson and Baldocchi [2001]; Comparing independent estimates of carbon dioxide exchange over 5 years at a deciduous forest in the southeastern United States; *Journal of Geophysical Research*, Volume 106, No. D24, 34, 176 – 34, 178.
- Yi *et al.* [2000]; Influence of advection on measurements of the net ecosystem-atmosphere exchange of CO<sub>2</sub> from a very tall tower; *Journal of Geophysical Research*, 105(D8), 9991– 9999.

A complete list of all KNMI -publications (1854 – present) can be found on our website

[www.knmi.nl/knmi-library/knmipub\\_en.html](http://www.knmi.nl/knmi-library/knmipub_en.html)



The most recent reports are available as a PDF on this site.

